UNIVERSIDADE FEDERAL DE MINAS GERAIS

ESCOLA DE ENGENHARIA

DEPARTAMENTO DE ENGENHARIA NUCLEAR

PÓS-GRADUAÇÃO EM CIÊNCIAS E TÉCNICAS NUCLEARES

JÉSSICA ACHILLES PIMENTEL

SPENT FUEL POOL ANALYSIS FOR A PWR USING DIFFERENT NUCLEAR FUELS

Belo Horizonte

2019

JÉSSICA ACHILLES PIMENTEL

SPENT FUEL POOL ANALYSIS FOR A PWR USING DIFFERENT NUCLEAR FUELS

Final Version

Master thesis submitted to the *Departamento de Engenharia Nuclear da Universidade Federal de Minas Gerais* in partial fulfillment of the requirements for the degree of Master of Science in Nuclear Science and Techniques.

Concentration Area: Nuclear and Energy Engineering

Advisor: Prof.ª Dr.ª Maria Auxiliadora Fortini Veloso.

Co-advisor: Prof.ª Dr.ª Cláubia Pereira Bezerra Lima

Belo Horizonte

2019

Pimentel, Jéssica Achilles.
P644s Spent fuel pool analysis for a pwr using different nuclear fuels [recurso eletrônico] / Jéssica Achilles Pimentel. – 2019.
1 recurso online (101 f. : il., color.) : pdf.

Orientadora: Maria Auxiliadora Fortini Veloso.
Coorientador: Claubia P. Bezerra Lima.

Dissertação (mestrado) - Universidade Federal de Minas Gerais, Escola de Engenharia.

Bibliografia: f. 99-101.
Exigências do sistema: Adobe Acrobat Reader.

1. Engenharia nuclear - Teses. 2. Combustíveis nucleares - Teses. 3. Criticalidade (Engenharia nuclear) - Teses. 4. Radioatividade - Teses. 5. Reatores de água pressurizada - Teses. 6. Torio - Teses. I. Veloso, Maria Auxiliadora Fortini. II. Lima, Cláubia Pereira Bezerra. III. Universidade Federal de Minas Gerais. Escola de Engenharia. IV. Título.

CDU: 621.039(043)

Ficha catalográfica: Biblioteca Profº Mário Werneck, Escola de Engenharia da UFMG.

UNIVERSIDADE FEDERAL DE MINAS GERAIS

PROGRAMA DE PÓS-GRADUAÇÃO EM CIÊNCIAS E TÉCNICAS NUCLEARES

FOLHA DE APROVAÇÃO

SPENT FUEL POOL ANALYSIS FOR A PWR USING DIFFERENT NUCLEAR FUELS

JÉSSICA ACHILLES PIMENTEL

Dissertação submetida à Banca Examinadora designada pelo Colegiado do Programa de Pós-Graduação em CIÊNCIAS E TÉCNICAS NUCLEARES, como requisito parcial para obtenção do grau de Mestre em CIÊNCIAS E TÉCNICAS NUCLEARES, área de concentração ENGENHARIA NUCLEAR E DA ENERGIA.

Aprovada em 26 de agosto de 2019, pela banca constituída pelos membros:

Profa. Maria Auxiliadora Fortini Veloso - Orientadora
Departamento de Engenharia Nuclear - UFMG

Profa. Cláubia Pereira Bezerra Lima
Departamento de Engenharia Nuclear - UFMG

Prof. Carlos Eduardo Velasquez Cabrera
Departamento de Engenharia Nuclear - UFMG

Prof. Jean Anderson Dias Salomé
FUNEC

Dra. Graiciany de Paula Barros
CNEN/CDTN

Belo Horizonte, 26 de agosto de 2019.

ACKNOWLEDGEMENTS

I am forever grateful to my advisors, Claubia Pereira and Maria Auxiliadora who have entrusted me with this research.

I would like to thank my mom and dad, Soraia Achilles Pimentel and Marcelo de Salles Pimentel, for their daily encouragement.

Thanks also to all my colleagues from the Department of Nuclear Engineering, DEN/UFMG, my teachers professors and staff.

Finally, I would like to thank the sponsor of this research, FAPEMIG.

ABSTRACT

A spent fuel pool (SFP) of a typical Pressurized Water Reactor (PWR) was evaluated considering six types of fuels: standard PWR fuel, MOX, (Th-U)O_2-16%, (Th-U)O_2-19.5%, (TRU-Th)O_2 and (TRU-U)O_2 fuels. The following benchmarks: *MOX and UO_2 Phase IV-B Burn-up Credit Criticality Benchmark* as well as *Thorium Pin Cell Burnup Benchmark* were validated using SCALE 6.0 code with KENO-VI transport code in the CSAS6 sequence. Then, the dimensions of the modeled fuel assembly from the benchmark were used to evaluate burnup and depletion studies. The six fuel assemblies were submitted to a burnup of 16 GWd/teHM with three operating cycles consisting of 420 days full power over 3.61 years. Considering the core refueling configuration, a supercell model was adopted to validate the MOX and UO_2 fuels benchmark. The assemblies and supercells were irradiated in a PWR core and after irradiation, the fuel assemblies and supercells were inserted in the pool. Three different geometric arrangements considering the core refueling configuration for assemblies were designed into the pool. It was required to find the minimum pitch distance that would optimize the assemblies' disposition in the SFP keeping the system under the upper criticality limit. Based on the criticality analyses, radioactivity, decay heat as well as inhalation and ingestion radiotoxicity were also studied over 50 years in the pool. After that, the delayed neutron fraction for each assembly and supercell were compared using the NEWT code. The k_{inf} evolution and the delayed neutron fraction (DNF) for all fuels' assemblies and supercells were evaluated during the burnup and compared with the standard UO_2. It was shown that in no case the pool needed to be resized. The results also show that the DNF of the assemblies using reprocessed fuel is smaller than the standard fuel, which is due to the ^{239}Pu presence and the ^{233}U production, which contribute to the low values obtained for delayed fission neutron fraction. These lower values of DNF suggest that reactors fueled with (TRU-Th)O_2 or (TRU-U)O_2 assemblies are harder to control. In contrast, the use of UO_2-supercells in combination with other types of fuels can provide the burnup extension especially when transuranic fuels are used.

KEYWORDS: SCALE 6.0; reprocessed fuel; spent fuel pool; criticality calculation; multiplication factor; decay heat; radioactivity; inhalation radiotoxicity; ingestion radiotoxicity; supercell; delayed neutron fraction; nuclear reactor safety parameters.

RESUMO

Uma piscina de combustível irradiado (SFP) de um reator de água pressurizada (PWR) foi avaliada considerando seis tipos de combustíveis: combustível padrão PWR, MOX, (Th-U)O_2-16%, (Th-U)O_2-19,5%, (TRU-Th)O_2 e (TRU-U)O_2. Os seguintes benchmarks: *Phase IV-B Burn-up Credit Criticality benchmark* bem como o *Thorium Pin Cell Burnup Benchmark* foram validados usando o código SCALE 6.0 com código de transporte KENO-VI na sequência CSAS6. Em seguida, as dimensões do elemento combustível do benchmark foram usadas para avaliar os estudos de queima e evolução do combustível. Os seis elementos combustíveis foram submetidos a uma queima de 16 GWd/teHM com três ciclos de operação consistindo em 420 dias com potência total durante 3,61 anos. Considerando a configuração de recarga do núcleo, adotou-se um modelo de supercélula para validar o *MOX e UO_2 benchmark*. As supercélulas também foram irradiadas em um núcleo PWR e após a irradiação, foram inseridas na piscina de combustível irradiado. Três diferentes arranjos geométricos que levam em consideração a configuração de recarga para os elementos combustíveis foram projetados dentro da piscina. Foi necessário encontrar a distância mínima (pitch) que otimizaria a disposição dos elementos na piscina, mantendo o sistema sob o limite superior de criticalidade. Com base nas análises de criticalidade, a radioatividade, o calor de decaimento, bem como a radiotoxicidade por inalação e por ingestão também foram estudados ao longo de 50 anos dentro da piscina. Depois disso, a fração de nêutrons atrasados de cada elemento combustível e supercélula foi estudada usando o código NEWT e comparada com o combustível padrão UO_2. Foi demonstrado que, em nenhum caso, a piscina precisaria ser redimensionada. Os resultados mostram ainda que a fração de nêutrons atrasados (DNF) dos elementos combustíveis que usam material reprocessado é menor que o combustível padrão, o que se deve à presença de ^{239}Pu e à produção de ^{233}U, contribuindo para os baixos valores obtidos para a fração de nêutrons atrasados. Esses valores mais baixos de DNF sugerem que os reatores que utilizam elementos combustíveis de (TRU-Th)O_2 ou (TRU-U)O_2 são mais difíceis de serem controlados. Em contraste, o uso das supercélulas de UO_2 juntamente com outros tipos de combustíveis favorece a extensão da queima, principalmente quando combustíveis transurânicos são utilizados, viabilizando assim o uso dos mesmos no núcleo do PWR.

PALAVRAS-CHAVE: SCALE 6.0; combustível reprocessado; piscina de combustível irradiado; criticalidade; coeficiente de multiplicação; calor de decaimento; radioatividade; radiotoxicidade por inalação; radiotoxicidade por ingestão; supercélula; fração de nêutrons atrasados; parâmetros de segurança.

RELATED WORKS

Achilles J.P., Cardoso F., Faria V., Pereira C., Veloso M**., Criticality safety analysis of spent fuel pool for a PWR using UO_2, MOX, $(Th\text{-}U)O_2$ and $(TRU\text{-}Th)O_2$ fuels**, Brazilian Journal of Radiation Sciences, ISSN: 2319-0612, pp. 01-16, Brazil, 2019.

J. Achilles, F. Cardoso, V. F. Castro, C. Pereira, M. A. F. Veloso, **SPENT FUEL POOL ANALYSIS FOR A PWR USING REPROCESSED NUCLEAR FUELS BASED ON U, MOX, Th-U, TRU-Th and TRU-U**, ASSOCIAÇÃO BRASILEIRA DE ENERGIA NUCLEAR – ABEN, International Nuclear Atlantic Conference – INAC, Brazil, 2019.

APPENDED PAPERS

Raoni A. S. Jonusan1, Dario M. Godino, J. Achilles, Santiago F. Corzo, Damian E Ramajo, Antonella L. Costa and Claubia Pereira, **Heat Transfer simulation in a Spent Nuclear Fuel Repository using ANSYS and OPENFOAM©**, ASSOCIAÇÃO BRASILEIRA DE ENERGIA NUCLEAR – ABEN, International Nuclear Atlantic Conference – INAC, Brazil, 2019.

Fernando P. Faria, Jéssica Achilles, Dario M. Godino, F. S. Corzo, D. E. Ramajo, F. Cardoso, Antonella L. Costa and Claubia Pereira**, Heat Transfer in a Simulated Spent Fuel Pool – A Comparision Between ANSYS and OPENFOAM© Codes,** ASSOCIAÇÃO BRASILEIRA DE ENERGIA NUCLEAR – ABEN, International Nuclear Atlantic Conference – INAC, Brazil, 2019.

Marcelo S. Ferreira, Pedro A. Rezende, João G. O. Marques, R. A. S. Jonusan, Jessica A. Pimentel, Antonella L. Costa, Claubia Pereira, **Overview on Nuclear Propulsion Systems For Space Exploration**, ASSOCIAÇÃO BRASILEIRA DE ENERGIA NUCLEAR – ABEN, International Nuclear Atlantic Conference – INAC, Brazil, 2019

LIST OF FIGURES

LIST OF TABLES

LIST OF ABBREVIATIONS AND ACRONYMS

BNFL – British Nuclear Fuels Ltd.

BOL – Beginning of Life.

CAPES – Coordenação de Aperfeiçoamento de Pessoal de Nível Superior.

CNEN – Comissão Nacional de Energia Nuclear.

CNPq – Conselho Nacional de Desenvolvimento Científico e Tecnológico.

DEN/UFMG – Departamento de Engenharia Nuclear/Universidade Federal de Minas Gerais.

DNF – Delayed Neutron Fraction.

DTLR – Departament for Transport. Local Government and the Regions.

ENDF – Evaluated Nuclear Data File.

EOC – End of Cicle.

FAPEMIG - Fundação de Amparo à Pesquisa do Estado de Minas Gerais.

FSAR – Final Safety Analysis Report.

GRS – Gesellscharft fur Anlagen und Reaktorsicherheit.

HM – Heavy Metal.

IAEA – International Atomic Energy Agency.

INEEL – Idaho National Engineering and Environmental Laboratory.

JAERI – Japan Atomic Energy research Institute.

JEFF – Joint Evaluation Fission and Fusion.

JEF – Joint Evaluation Fission.

JENDL – Japanese Evaluated Nuclear Data Library.

LWR – Light Water Reactor.

MIT – Massachusetts Institute of Technology.

MOX – Mixed Oxide Fuel.

NEWT_238 – NEWT using 238-groups energy libraries.

NUPEC – Nuclear Power Engineering Center.

OECD – Organization for Economic Co-operation and Development.

ORIGEN – Oak Ridge Isotope Generation and Depletion.

ORNL – Oak Ridge National Laboratory.

PSI – Paul Scherrer Institute.

PUREX – Plutonium-uranium redox extraction.

PWR – Pressurized Water Reactor.

RSD – Relative Standard Deviation.

SCALE – Standardized Computer Analyses for Licensing Evaluations.

SD – Standard Deviation.

SFP – Spent Fuel Pool.

(Th-U)O_2 – Thorium-Uranium Dioxide.

(TRU-Th)O_2 – Transuranic-Thorium Dioxide.

(TRU-U)O_2 – Transuranic-Uranium Dioxide.

UFMG – Universidade Federal de Minas Gerais.

UO_2 – Uranium Dioxide.

UREX – Uranium redox extraction.

Zr-2 – Zircaloy-2.

LIST OF SYMBOLS

β_{eff} – Effective delayed neutron fraction.

Bq – Becquerel.

atoms/cm³ – Atomic density.

g/cm³ – Density.

GWd/TeHM - Gigawatts days per Metric Ton of Heavy Metal.

K – Kelvin.

k_{inf} – Infinity multiplication factor.

m³.air – cubic meters per air.

m³.water – cubic meters per water.

mm – Millimeter.

Watt/ton – Watts per Ton of Heavy Metal.

pcm – Per cent mille.

w/o – Weight fraction.

Table of contents

1. INTRODUCTION

Management of spent fuel arising from nuclear power production has long been considered an important issue due to the political, economical, and societal implications associated with it. In view of the large amount of spent fuel being progressively added to the cumulative inventory in the world, the significance of spent fuel management will continue to grow in the future [1].

During the past 50 years, most of nuclear power has been produced by Light Water Reactors (LWR) using UO_2 as fuel in a once through fuel cycle. The high rate of uranium consumption makes the natural resource of this fuel limited to this century even at the high cost of uranium ore [2]. Beside this, after several decades of commercial operating of nuclear power plants for electricity generation, a significant amount of by products containing fissile and/or fertile materials has been accumulated worldwide. Between them, the quantity of plutonium has been allocated to a utility, therefore, the interest ts to recycle it in the form of MOX fuel assemblies as soon as possible, not only to avoid the high storage charges but also because of the degradation over time of its isotopic quality [3].

To decrease the utilization of uranium, many nuclear facilities are planning, or have already implemented plutonium recycling schemes in thermal reactors, principally PWRs. Plutonium is normally recycled and mixed with depleted uranium as Mixed Oxide (MOX) in the form of plutonium dioxide (PuO_2) in the same reactors [4]. The fresh uranium consumption of nuclear energy systems of current generation could be reduced by 50% through reprocessing spent fuel following by recycling of the retrieved uranium and plutonium rather than adopting the once-through fuel cycle [3]. Another option is the utilization of (thorium/uranium or thorium/plutonium or thorium/transuranic or transuranic/uranium) oxide as a mixed fuel [4-8].

There is no big difference of physical properties and irradiation behaviors between MOX fuel and UO_2 fuel, because Pu content of MOX fuel for Pu thermal utilization is low and experiences have been shown that security and operation of the reactors using MOX fuel can achieve a considerable

performance compared with the UO_2 fuel. This is because Pu content in the MOX fuel for light water reactors (LWRs) is low compared to MOX fuel for fast reactors [9,10].

It is prudent to recover the fissile material left in the spent fuel for reuse by reprocessing, therefore it reduces the requirement of fresh materials. Also, this reduces the volume of radioactive waste to be disposed off for the same amount of power production [11].

In the early eighties, France implemented a closed nuclear fuel cycle policy reprocessing the spent fuel and recycling the fuel obtained from Pu spiked with depleted uranium (MOX) inserting it in its reactors. Such a policy was also adopted by other European countries and by Japan [12].

More recently, many researchers turned their attention to Th fuel cycles in PWRs aiming at reducing the generation of minor actinides, at improving the nuclear power sustainability, and at better fuel utilization and breeding [13-15]. Similarly, International Atomic Energy Agency (IAEA) and Nuclear Energy Agency (NEA) have presented studies about the possible role of Th utilization in power reactors and the associated fuel cycles [16, 17]. These studies were interested in assessing the feasibility of using ^{233}U-Th fuels in PWR without worrying about how to obtain the initial ^{233}U fuel load or the transition from uranium to thorium cycle in the current nuclear power plants.

Based on the idea of the adoption of the closed fuel cycle in the current PWRs, the goal in this work is to evaluate, considering neutronics aspects, if there will be needed to change the spent fuel pool (SFP) design when extending the use thorium based fuels and reprocessed fuels. Furthermore, radioactivity, heat decay, inhalation and ingestion radiotoxicity as well as the delayed neutron fraction analysis for these fuels, were studied over 50 years in the spent pool.

In the academic environment and in nuclear power plants, the computational simulations have enormous importance, either to study behavior of materials or to analyze safety parameters. Given the importance of the safety parameters inside the nuclear simulation, this work aims to validate the model used by Departamento de Engenharia Nuclear - DEN at Universidade Federal de Minas Gerais - UFMG using the SCALE 6.0 nuclear code system.

The SCALE Code System is a widely used modeling and simulation for nuclear safety analysis and design that is developed, maintained, tested, and managed by the Reactor and Nuclear Systems Division (RNSD) at Oak Ridge National Laboratory (ORNL) [18]. It is a validated code system that provides a comprehensive, verified and validated, which have a friendly tool set for criticality safety, reactor physics, spent fuel characterization, radiation shielding, and sensitivity and uncertainty analysis [19].

Among SCALE6 modules, there are two main control modules that were used frequently in this work, the CSAS6 (Criticality Safety Analysis Sequence) for criticality calculations and the TRITON (Transport Rigor Implemented with Time-dependent Operation for Neutronic depletion) for transport and depletion calculations [20, 21].

Both sequences prepare cross section data to be used for neutron transport code, by using the Monte Carlo KENO-VI transport code or the deterministic neutron transport NEWT code [22].

The CSAS6 control module contains criticality safety analysis sequences using the KENO-VI module for multidimensional models with more complex geometries, including hexagonal arrays. Sequences that provide problem-dependent multigroup cross sections for use in stand-alone codes are also available in the CSAS5 module. Both modules perform the criticality calculation with SCALE 6.0. On the other hand, the NEWT code only can use collapsed cross sections [22].

The TRITON control module was used for the fuel evolution calculations. It was developed in conjunction with KENO-VI and ORIGEN-S and allows fuel evolution calculations. It can be used to automatically process 28 cross-section dependent problems followed by the multiplication factor (k) calculation for a two-dimensional configuration using KENO-VI and, through ORIGEN-S, make the depletion calculations to predict isotopic concentrations, source term and heat decay, with flow variation over time either deterministically in 2-D or stochastic in 3-D [21]. When using TRITON, cross section processing modules and neutron transport code are called, and again, it can be by KENO-VI or NEWT, and then TRITON perform the communication with depletion code ORIGEN-S [23].

The NEWT is a deterministic code and considers two-dimensional (2D) geometry. Therefore, NEWT perform criticality calculations using collapsed energy groups. Jointly with the infinite multiplication factor, NEWT can calculate the effective delayed neutron factor and decay constant per precursor group [20].

Based on the idea of the adoption of the closed fuel cycle in the current PWRs, the goal in this study is to evaluate, considering neutronics aspects, if there will be needed to change the spent pool design when extending the use thorium based fuels and reprocessed fuel assemblies in the PWR core.

Six types of fuels were selected based on previous studies and validations from the Departamento de Engenharia Nuclear - DEN at Universidade Federal de Minas Gerais – UFMG: standard PWR fuel, mixed oxide (MOX), thorium (Th-U)O_2 with 16 and 19.5 w/o fissile material, reprocessed transuranic fuel spiked with thorium (TRU-Th)O_2 and transuranic fuel spiked with uranium (TRU-U)O_2. MOX and UO_2 fuels compositions have been derived following Phase IV-B Burn-up Credit Criticality benchmark [24] while (Th-U)O_2 fuel has its composition taken from Thorium Pin Cell Burnup Benchmark [25].

Considering the supercells arrangement also described in the Burnup Credit benchmark, the study was after extended. Hence, to perform the analysis, important nuclear safety parameters are going to be analyzed, some of which are: infinite nuclear multiplication factor - k_∞, radioactivity, heat decay, inhalation and ingestion radiotoxicity as well as effective delayed neutron fraction (β_{eff}) and decay constant (λ).

The chapters division of this work was implemented in a way that the next chapter presents the benchmarks description followed by the methodology performed to complete the validations considering criticality and depletion situation.

Therefore, chapter three comprehends the all six fuel assemblies' description setting all assembly compositions. The reprocessed transuranic fuel spiked with thorium was obtained from some

studies developed at Departamento de Engenharia Nuclear DEN/UFMG [26, 27] adjusted to obtain the same neutron multiplication factor at begin of life (BOL). Next, in chapter four, the burnup results will be performed using the TRITON module.

In chapter five, a close analysis of the nuclear power plants was made in order to ensure a safety project. For this, the criticality safety analysis, decay heat, radiotoxicity, as well as, inhalation and ingestion radiotoxicity for all fuels' assemblies were performed over 50 years in the spent fuel pool, based on the Angra II pool described at Safety Analysis Report - FSAR [28].

Furthermore, chapter six comprehends the MOX and UO_2 benchmark extension using the validated supercell mode. The burnup criticality calculations, as well as, criticality safety analysis under the spent fuel pool were performed for two different configurations of UO_2-supercell. Chapter seven uses the deterministic method, with NEWT module to address the study of the delayed neutron fraction and the decay constant variation over the burnup. Finally, chapter eight covers the general conclusions, some future perspectives and opportunities are discussed.

2. MODEL VALIDATION

The criticality study was carried out so that the methodology used in this work was validated using compositions from different nuclear fuels in a PWR system. Afterward, the safety parameters as well as the criticality analysis for those fuels were assessed using the spent fuel pool model.

Therefore, two benchmarks were used to compare with the developed model in this work. The one using MOX fuel; *Burn-up Credit Criticality Benchmark. Phase IV-B: Results and Analysis of MOX Fuel Depletion Calculations* [24] and another with (Th-U)O_2 fuel; *A PWR Thorium Pin Cell Burnup Benchmark* [25]. The benchmarks were used to compare with the developed model in this work using the SCALE 6.0 code.

For this analysis, the following steps were adopted:

- Fuel assemblies modelling following the benchmarks;
- Benchmarks methodology validation;
- Criticality analysis, burnup and fuels depletion;
- Spent fuel pool modelling according to the Angra 2 pool;
- Analysis of criticality, decay heat, radioactivity, inhalation and ingestion radiotoxicity into the spent fuel pool;
- Supercells modelling, validation and depletion;
- Delayed Neutron Fraction evaluation.

The continuous energy library, ENDF/BVII collapsed of 238 groups was used for the fuels depletion. Therefore, the results obtained for each fuel (MOX, thorium based fuels with 16% and 19.5% of fissile material, (TRU-Th)O_2 with 10% fissile material and (TRU-U)O_2 with 12.5% fissile material) were compared with the results obtained for the standard UO_2 fuel.

Eight participants from seven countries undertook the calculations for the Phase IV-B Burn-up Benchmark [24]. To identify the impact of different nuclear data on the steady-state criticality calculation, the Average, Standard Deviation (SD) and Relative Standard Deviation (RSD) of k_{inf} were calculated using the equations below:

$$\text{Average} = \frac{1}{L} \sum_{i=1}^{I} k_l \quad (1)$$

$$SD = \sqrt{\frac{\sum_{l=1}^{L} (k_l - \text{Average})^2}{L}} \quad (2)$$

$$\text{RSD} = \frac{\text{SD}}{\text{Average}} \quad (3)$$

Where L represents the number of participants/number of libraries and k_l the infinite nuclear multiplication factor for each participant/library.

The geometry and composition descriptions used in the benchmarks are presented in the following sections, as well as, the compared results with DEN/UFMG.

2.1. MOX AND UO_2 BENCHMARK DESCRIPTION

The investigation of burnup credit for mixed oxide (MOX) fuel containing a mixture of uranium and plutonium oxides was an ongoing objective of the Phase IV-B Burn-up Credit Criticality Benchmark. The proposed MOX fuel selected by the benchmark followed the study of burnup credits methods for a mixed UO_2-MOX PWR core [24].

The MOX fuel adopted for the benchmark derived from the reprocessing of thermal reactor UO_2 fuels. This exercise is based upon fuel compositions provided by the benchmark organizers and considered the impact of different initial plutonium isotopic compositions in the MOX fuel, associated with first-generation MOX recycle. The MOX assembly pre-irradiation fuel composition is shown in Table 1.

Table 1 – Initial MOX fuel compositions [24]

Nuclide	Atoms/barn.cm for given fuel pin			
	High	**Medium**	**Low**	**Average (for pin cell calculation)**
^{234}U	2.5718E-07	2.6436E07	2.6789E-07	2.5952E-07
^{235}U	5.3798E-05	5.5300E-05	5.6040E-05	5.4287E-05
^{238}U	2.1194E-02	2.1786E-02	2.2077E-02	2.1387E-02
^{238}Pu	4.1677E-05	3.6128E-05	2.8473E-05	4.6610E-05
^{239}Pu	1.1259E-03	7.8717E-04	6.2038E-04	1.0156E-03
^{240}Pu	5.3500E-04	3.7403E-04	2.9478E-04	4.8255E-04
^{241}Pu	1.9392E-04	1.3557E-04	1.0685E-04	1.7491E-04
^{242}Pu	1.4636E-04	1.0233E-04	8.0644E-05	1.3201E-04
O	4.6602E-02	4.6553E-02	4.6529E-02	4.6586E-02

In Phase IV-B Benchmark, the same geometry related to a typical PWR assembly with 3.6568 m of height and 1.26 cm of pitch distance was adopted for MOX and UO_2 fuels. The assembly geometry with reflective boundary conditions was considered. A reduced density zircaloy has been specified for the fuel pin and no air gap between fuel and cladding is assumed [24]. The 24 guide tubes and one instrumented tube were modelled as water-filled zircaloy-2 tubes [24]. The same geometry using reflective boundary conditions was adopted for all the six fuels investigated in this work.

The Pin cell dimensions are presented in Figure 1. The assembly dimensions and the non-fissile material compositions are specified in Table 2 and Table 3 [24].

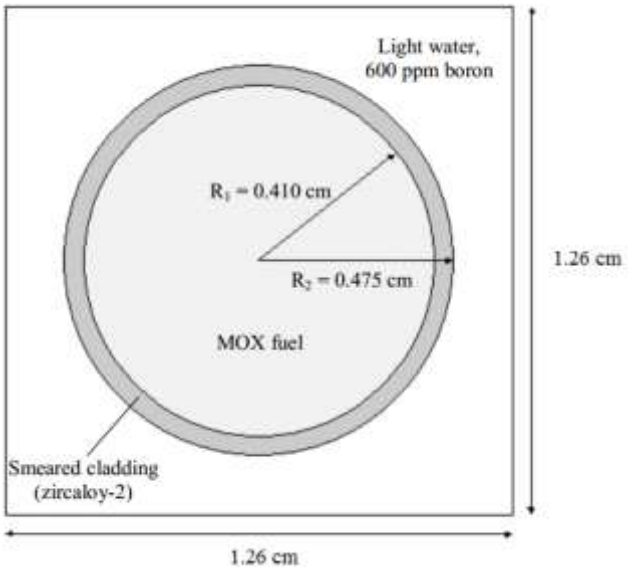

Figure 1 – MOX Pin Cell [24].

Table 2 – Fuel model parameters considering guide and instrumented tubes dimensions [24]

Parameter	**Dimention (cm)**
Fuel pin pitch	1.26
Fuel pin radius	0.475
Fuel pellet radius	0.410
Cladding thickness	0.065
Guide tube outer radius	0.613
Guide tube inner radius	0.571
Wall thickness	0.042

Table 3 – Non-fissile material compositions [24]

Nuclide	Atoms/barn.cm
Zircaloy-2 (5.8736 g/cm³ - reduced density)	
Zr	3.8657E-02
Fe	1.3345E-04
Cr	6.8254E-05
Coolant/moderator (600 ppm boro, 0.7245 g/cm³)	
H	4.8414E-02
O	2.4213E-02
^{10}B	4.7896E-06
^{11}B	1.9424E-05

The MOX fuel assembly geometry adopted is a 17 x 17 PWR fuel assembly with three enrichment zones, as shown in Figure 2. The initial MOX enrichments for these zones are summarized in Table 4 [24].

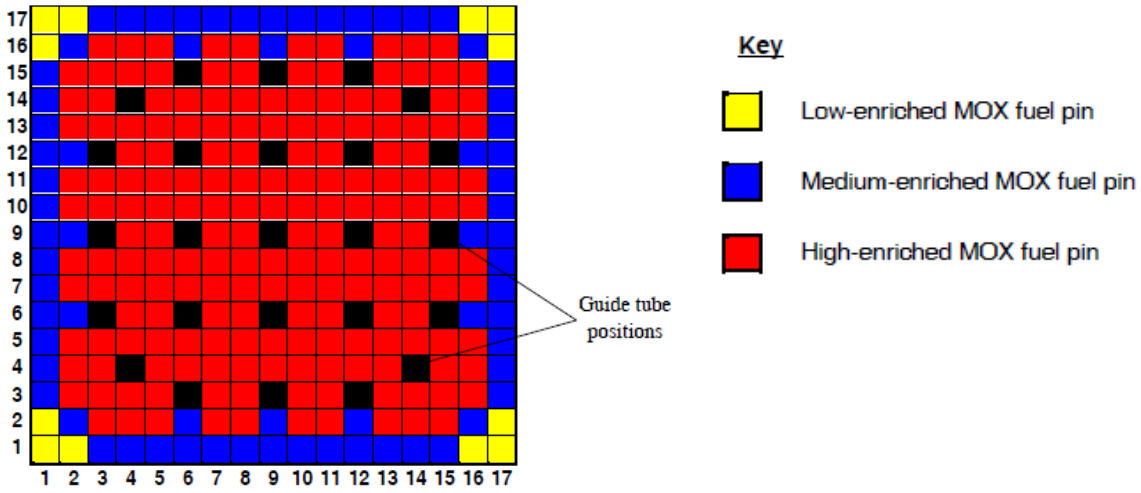

Figure 2 – MOX fuel assembly [24]

Table 4 Initial MOX fuel enrichment [24]

MOX fuel case A (First recycle MOX)	**MOX fuel enrichment, w/o $Pu_{fissile}$/[U+Pu]**
High	5.692
Medium	3.984
Low	3.142
Average	5.136

The UO_2 fuel assemblies have an initial enrichment of 4.3 w/o $^{235}U/U$ taken from the Phase IV-B Benchmark [24]. The same fuel assembly geometry adopted for the MOX fuel in the benchmark was also adopted for the UO_2 fuel, following the typical 17 x 17 PWR assembly. The initial composition for the UO_2 fuel is presented in Table 5 [24].

Table 5 – Initial composition for 4.3 w/o $^{235}U/U$ UO_2 fuel [24]

Nuclide	**Atoms/barn.cm**
^{234}U	8.1248E-06
^{235}U	1.0113E-03
^{236}U	8.0558E-06
^{238}U	2.2206E-02
O	4.6467E-02

As for the irradiation history, three operating cycles are requested; two cycles consisting of 420 days full power with end of cycle (EOC) burnup equal to 16 GWd/teHM followed by 30 days downtime, and one cycle consisting of 420 days full power with EOC burnup equal to 16 GWd/teHM. The material temperatures are specified in Table 6 [24].

Table 6 – Material temperatures [24]

Material	**Temperature (K)**
Fuel temperature	900
Cladding temperature	620
Coolant/moderator temperature	575

2.2. MOX AND UO_2 BENCHMARK VALIDATION

The benchmark validation for MOX and UO_2 fuels was performed using KENO-VI sequence making use of CSAS6 module in the SCALE6.0 code and ENDF/B-VII collapsed 238-energy-group library using the same irradiation history used in Phase IV-B benchmark [24]. The MOX and UO_2 benchmark results were compared with the results obtained in this present study. The fuel assemblies were modeled using the same geometry data and materials provided by the benchmark.

Table 7 summarizes the three operating cycles, the end of cycle 1, end of cycle 2 and the end of cycle 3 (EOC 1, EOC 2 and EOC 3) considering the values obtained for k_{inf}, as well as Average, SD and RSD calculations for the eight groups that contributed for the MOX and UO_2 benchmark, as well as, DEN/UFMG values.

Table 7 – k_{inf} and reactivity change for all benchmark participants and DEN/UFMG

Participant		k_{inf}			Absolute difference in pcm		
		EOC 1	EOC 2	EOC 3	EOC 1	EOC 2	EOC 3
NUPEC		1.05978	1.00753	0.96100	205	454	598
CEA		1.05624	0.99968	0.94869	149	331	633
GRS		1.05910	0.99909	0.94752	137	390	750
PSI		1.06088	1.00618	0.95837	315	319	335
BNFL		1.04976	0.99654	0.94974	797	645	528
JAERI		1.05541	0.99749	0.95292	232	550	210
DTLR		1.05900	1.00460	0.95100	127	161	402
ORNL		1.06269	1.01166	0.96610	496	867	360
DEN/UFMG		1.0567	1.0041	0.9598	103	111	478
Average	Before	1.05786	1.00108	0.95442			
	Updated	1.05773	1.00298	0.95502			
SD	Before	0.00402	0.00543	0.00667			
	Updated	0.00357	0.00481	0.00612			
RSD (%)	Before	0.38	0.54	0.70			
	Updated	0.33	0.47	0.64			

Table 7 presents the selected cases using different libraries to proceed with the validation jointly to the k_{inf} absolute difference ($|k_{inf}$ Result - k_{inf} Average$|$). The results addressed as BEFORE do not consider the k_{inf} results from this work while the results referred to as UPDATED contemplate results from DEN/UFMG. It is observed a decrease in multiplication factor standard deviation and multiplication factor relative standard deviation validating thus, the procedure adopted. Table 8 summarizes the participants with their analysis methods including neutron data code and library.

Table 8 – Benchmark participants and reactivity change analysis methods [24]

Participant	**Institution**	**Neutron data processing Code**	**Neutron data Library**
NUPEC	Nuclear Power Engineering Center	CASLIB	E4LBL70 based on ENDF/B-IV
CEA	CEA/DRN	NJOY from JEF-2 file	CEA-93 based on JEF-2.2 evaluations
GRS	Gesellschaft fur Anlagen und Reaktorsicherheit	RESMOD/HAMMER	292-group library JEF-2.2
PSI	Paul Scherrer Institute	BOXER	JEF-1
BNFL	British Nuclear Fuels Ltd	WIMS8A – NJOY & WILT	172-group
JAERI	Japan Atomic Energy Research Institute	SWAT / SRAC	JENDL-3.2
DTLR	Departament for Transport, Local Government and the Regions	WIMS	JEF-2.2
ORNL	Oak Ridge National Laboratory	BONAMI/NITAWL	238-energy-group
DEN/UFMG	Department of Nuclear Engineering	NEWT/ORIGEN-S	V7-238-energy-group

2.3. THORIUM PIN CELL BENCHMARK DESCRIPTION

The work reported in Thorium Pin Cell Burnup Benchmark [25] involves analysis of a PWR pin cell excised from a standard 17x17 assembly typical of large Westinghouse PWRs. The usual all-UO_2 fuel pellets were replaced by a (Th-U)O_2 mixture at 94% of theoretical density consisting of 75w/o Th, 25 w/o U on a heavy metal basis, with the later enriched to 19.5 w/o ^{235}U, to give an overall enrichment of 4.869 w/o ^{235}U in total heavy metal. The pin cell model representing the unit

lattice cell of a Westinghouse PWR fuel bundle and used for the Thorium Benchmark burnup calculations is shown in Figure 3.

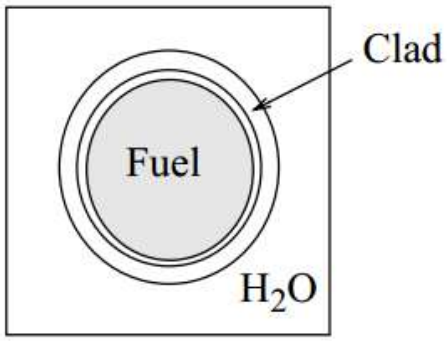

Figure 3 – The pin cell model of a Westinghouse PWR [25].

Tables 9 and 10 show detailed parameters of the pin cell model for a Westinghouse PWR assembly. Parameters at hot full power were used in the benchmark calculations.

Table 9 – Pin Cell Model Parameters [25]

Parameter	**Hot Full Power**
Fuel Temperature (K)	900
Power density (KW/KgHM)	38.1347
Power density (KW/liter cell)	107.284
Fuel density (g/cm³)	9.424
Cladding Temperature (K)	621.1
Cladding density (g/cm³)	6.505
Coolant Pressure (bars)	155.13
Coolant temperature (K)	583.1
Coolant density (g/cm³)	0.705
Fuel pellet Radius (mm)	4.1274
Cladding Inner Radius (mm)	4.1896
Cladding Outer Radius (mm)	4.7609
Pin Pitch (mm)	12.626

Table 10 – Initial fuel compositions at Hot Full Power Conditions [25]

	Nuclide	Atoms/barn.cm
Fuel	^{232}Th	1.61215E-02
	^{234}U	8.24518E-06
	^{235}U	1.03615E-03
	^{238}U	4.22957E-03
	^{16}O	4.26865E-02
Coolant	^{1}H	4.8414E-02
	^{16}O	2.4213E-02

2.4. THORIUM PIN CELL BENCHMARK VALIDATION

Following the same irradiation history presented by the A PWR Thorium Pin Cell Burnup Benchmark [25], with power density of 38.1347 kW/kgHM for 1320 days, the results obtained in this work (DEN/UFMG) were compared with the results obtained for the institutions MIT and INEEL in the benchmark. The simulations were performed to validate the thorium benchmark using the SCALE 6.0 code. The pin cell model was modeled using the same geometry data and materials taken from the Thorium Benchmark. Figure 4 shows the modeled pin cell.

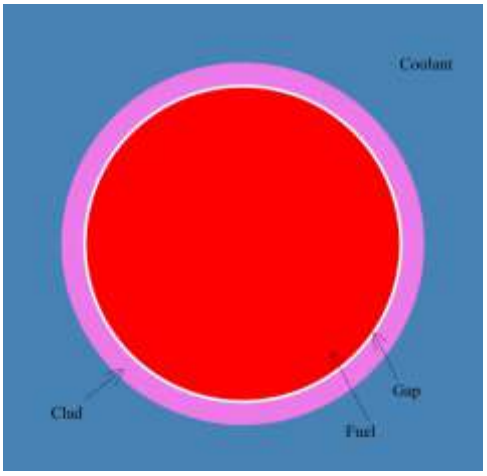

Figure 4 – Thorium Pin Cell modelled [author]

For the infinite multiplication factor calculation, the CSAS6 sequence was used considering 5000 particles and 243 generations. The values obtained for k_{inf}, as well as, the values presented in the benchmark, Average, SD and RSD, including the code and library used for each institution are presented in Table 11.

Table 11 – Comparison of k_{inf} values using different codes and cross section libraries

Country	Institute/Department	Code	Library	k_{inf}
USA	MIT[1]	CASMO-4	ENDF/ B-VI	1.23782
USA	MIT	MOCUP	UTXS	1.23354
USA	INEEL[2]	MOCUP	UTXS	1.22347
BRAZIL	DEN/UFMG[3]	MCNP5	ENDF/B-VII 09c	1.23009
BRAZIL	DEN/UFMG	SERPENT	ENDF/B-VII 09c	1.24194
BRAZIL	DEN/UFMG	MCNP5	ENDF/B-VII 12c →WT	1.22857
BRAZIL	DEN/UFMG	SERPENT	ENDF/B-VII 12c → WT	1.22492
BRAZIL	DEN/UFMG	MCNP5	ENDF/B-VII NJOY99	1.23517
BRAZIL	DEN/UFMG	SERPENT	ENDF/B-VII NJOY99	1.23404
BRAZIL	DEN/UFMG	KENO-VI	238 group (v7-237)[4]	1.2429 ±0.0016
Average	Before Updated		1.23267 1.23370	
SD	Before Updated		0.00516 0.00578	
RSD	Before Updated		0.42% 0.47%	

→ it indicates the use of temperature correction.

[1] Massachusetts Institute of Technology – MIT [25]

[2] Idaho National Engineering and Environmental Laboratory – INEEL [25]

[3] Departamento de Engenharia Nuclear – DEN/UFMG

[4] Collapsed from ENDF/B-VII

The values obtained for DEN/UFMG are again in accordance with the thorium benchmark values using different libraries and thus, the procedure adopted was validated.

The selected library was ENDF / B-VII collapsed in 238 groups (V7-238), once that presents the standard deviation close to the other institutions libraries, besides that, it is the collapsed version of the most updated continuous library, containing cross section data of 148 groups fast nuclides and 90 groups of thermal nuclides [23].

3. (Th-U)O_2-16%, (TRU-Th)O_2 AND (TRU-U)O_2 FUELS

In this work, two benchmarks are considered. However, the safety parameters and criticality analysis are assessed for six different fuels. The MOX and UO_2 fuel composition and assembly geometry have been derived from the Phase IV-B Benchmark [24] while the (Th-U)O_2 fuel enriched to 19.5 w/o ^{235}U composition was taken from the Thorium Benchmark [25]. The (Th-U)O_2-16%, (TRU-Th)O_2 and (TRU-U)O_2 fuel compositions were obtained after successive simulations been performed. All fuel assembly geometries were derived from the Phase IV-B benchmark.

Following the Thorium Benchmark methodology, successive simulations were performed using the SCALE 6.0 code in the KENO-VI module, varying the ^{235}U percentage from 2% to 19% in the thorium fuel. Then, the thorium fuel with 16 w/o ^{235}U/U, giving an overall enrichment of 3.765 w/o ^{235}U in total heavy metal basis was chosen to be studied once that it has the infinite multiplication factor of neutrons as close as possible to the k_{inf} obtained for the MOX fuel taken from the Phase IV-B Benchmark. The (Th-U)O_2-16% fuel also consists of a mixture at 94% of theoretical density, with 75 w/o consisting of thorium and 25 w/o of uranium. Table 12 shows the initial composition in atoms/barn.cm for the (Th-U)O_2-16% fuel.

Table 12 – Initial (Th-U)O_2-16% fuel composition [author]

	Isotope	**Atoms/barn.cm**
Fuel	^{232}Th	1.61215E-02
	^{234}U	8.24518E-06
	^{235}U	8.52488E-04
	^{238}U	4.41091E-03
	^{16}O	4.26835E-02

For the characterization of the reprocessed transuranic fuel, denominated (TRU-Th)O_2 and (TRU-U)O_2, the composition of a UO_2 fuel of a typical PWR, with an initial enrichment of 3.1% with 33 GWd/teHM of burnup, after 5 years in cooling pool was considered [27]. Then, it was theoretically

reprocessed by UREX+ technique. The first stage involves the recuperation of uranium, plutonium, curium and neptunium. With this stage, 99.99% U, 99.5% Pu, 71% Np, 98% Am and 79% of Cm were recovered.

The reprocessed (TRU-Th)O_2 fuel was then spiked with ^{232}Th and the (TRU-U)O_2 spiked with uranium and the amount of fissile material contained therein being varied; starting at 1% and increasing to 30%. The (TRU-Th)O_2 fuel composition was obtained after successive simulations and verified that a 73.8 w/o Th spiked, gives an overall fissile material of 10 w/o in this fuel. For the (TRU-U)O_2 fuel, 0.2 w/o ^{235}U in total heavy metal basis gives an overall 12.5 w/o fissile material, ensuring, for both fuels, an infinite multiplication factor as close as MOX fuel's k_{inf} presented in the Phase IV-B Benchmark. Tables 13 and 14 show the initial composition in atoms/barn.cm for the (TRU-Th)O_2 and (TRU-U)O_2 fuels.

Table 13 – Initial (TRU-Th)O_2 fuel compositions [author]

Isotope	**Atoms/barn.cm**
Th-232	7.3848E-01
Np-235	2.2837E-12
Np-236	5.3151E-09
Np-237	4.6381E-03
Np-238	1.8087E-12
Np-239	1.1620E-09
Pu-236	6.2732E-09
Pu-237	2.8747E-21
Pu-238	2.4498E-03
Pu-239	7.1654E-02
Pu-240	3.0021E-02
Pu-241	1.6285E-02
Pu-242	8.5531E-03
Pu-243	1.4444E-18
Pu-244	5.7068E-07
Pu-246	5.4094E-24
Am-241	4.9653E-03
Am-242m	1.3292E-05
Am-242	1.5900E-10
Am-243	1.8689E-03
Cm-241	8.1851E-27
Cm-242	1.0782E-07
Cm-243	5.7228E-06
Cm-244	4.3062E-04
Cm-245	2.2711E-05
Cm-246	2.9233E-06
Cm-247	3.2156E-08
Cm-248	1.8776E-09
Cm-250	1.0220E-17

Table 14 – Initial (TRU-U)O_2 fuel compositions [author]

Isotope	Atoms/barn.cm
^{234}U	1.41578E-02
^{235}U	1.76973E-03
^{236}U	7.07892E-02
^{238}U	6.21175E-01
^{238}Pu	3.02688E-03
^{239}Pu	8.83277E-02
^{240}Pu	3.70418E-02
^{241}Pu	2.00221E-02
^{242}Pu	1.05417E-02
^{237}Np	5.71485E-03
^{241}Am	6.12583E-03
^{242m} Am	1.63848E-05
^{243}Am	2.30041E-03
^{242}Cm	1.32844E-07
^{243}Cm	7.05730E-06
^{244}Cm	5.30545E-04
^{245}Cm	2.79548E-05
^{246}Cm	3.59795E-06

Table 15 summarizes the initial k_{inf} obtained for the six fuels at beginning of life (BOL). The six analyzed fuels use the same 17x17 assembly geometry taken from Phase IV-B exercise [24].

Table 15 – k_{inf} for standard UO_2 and other fuels at Begin of Life (BOL)

Fuel	**k_{inf}**
MOX	1.1517 ± 0.0033
UO_2	1.3234 ± 0.0018
(Th-U)O_2-19.5%	1.2147 ± 0.0012
(Th-U)O_2-16%	1.1587 ± 0.0026
(TRU-Th)O_2	1.1525 ± 0.0010
(TRU-U)O_2	1.1553 ± 0.0011

3.1. FUEL ASSEMBLIES DESCRIPTION

As presented in Phase IV-B: Results and Analysis of MOX fuel Depletion Calculations, the MOX fuel enrichment average is 0.25 w/o ^{235}U/U, while the UO_2 fuel has an initial enrichment of 4.3 w/o ^{235}U/U. Following A PWR Thorium Pin Cell Burnup Benchmark, the (Th-U)O_2-19.5% fuel has an overall enrichment of 4.869 w/o ^{235}U in total heavy metal. The (Th-U)O_2-16% has 3.765 w/o ^{235}U in total heavy metal basis.

The (TRU-Th)O_2 fuel composition with different quantities of fissile material was obtained after successive simulations and it was found that a dilution of 73.8 w/o ^{232}Th gives an overall equivalent to 10 w/o fissile material. The (TRU-U)O_2 depleted fuel has 0.2 w/o ^{235}U in total heavy metal basis and an overall 12.5 w/o fissile material.

The multiplication factor desired should be approximately the same for MOX, (Th-U)O_2 16%, (TRU-Th)O_2 and (TRU-U)O_2 assemblies, following the Begin Of Life and Hot Zero Power of Phase IV-B Benchmark. Therefore the fissile material was set to reach the same multiplication factor for the other fuels, the (Th-U)O_2-19.5% at the Begin Of Life has a higher k_{inf} once that it follows the Thorium Benchmark. Figures 5 to 10 illustrate all the modelled fuel assemblies.

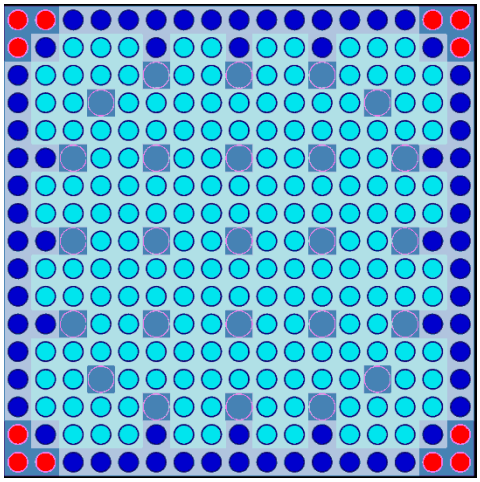

Figure 5 – MOX modelled assembly [author].

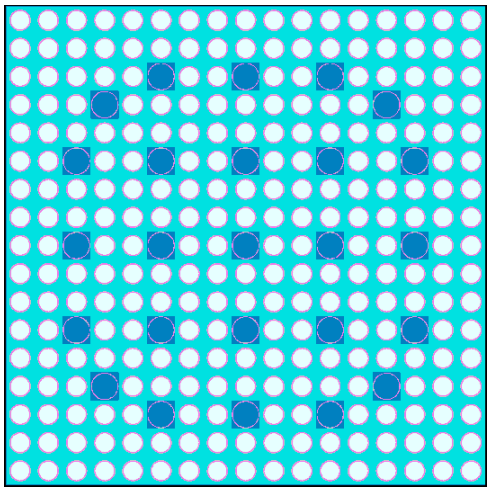

Figure 6 – UO_2 modelled assembly [author].

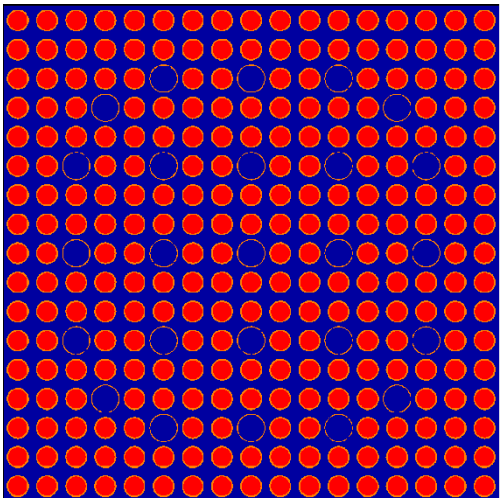

Figure 7 – (Th-U)O_2-19.5% modelled assembly [author].

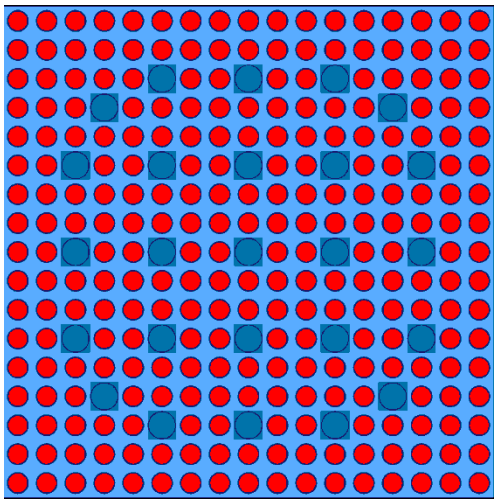

Figure 8 – (Th-U)O_2-16% modelled assembly [author].

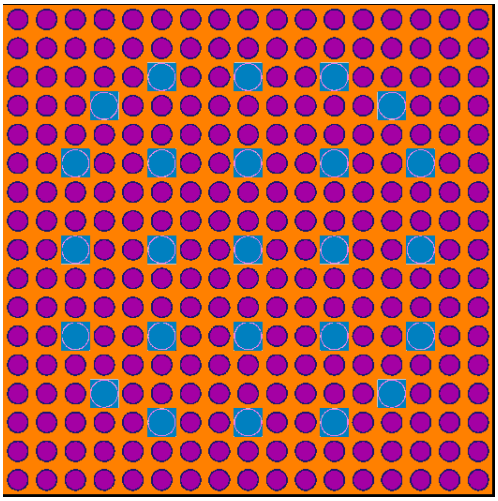

Figure 9 – (TRU-Th)O_2 modelled assembly [author].

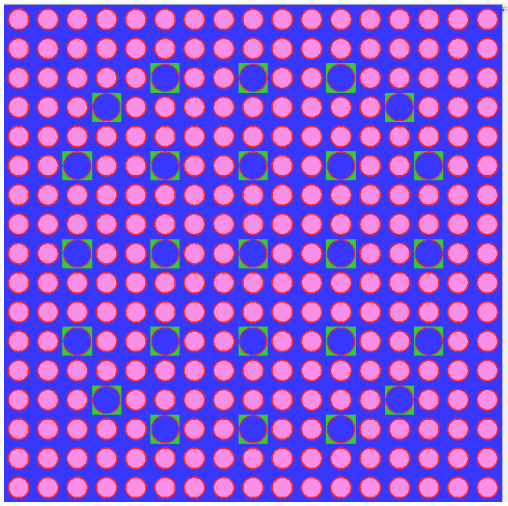

Figure 10 – (TRU-U)O_2 modelled assembly [author]

After the methodology validation, the fuel assemblies were inserted in the PWR system and the criticality was studied.

4. FUELS BURNUP RESULTS

After setting all assemblies composition, the burnup criticality calculations were performed for MOX, UO_2, (Th-U)O_2-19.5%, (Th-U)O_2-16%, (TRU-Th)O_2 and (TRU-U)O_2 fuels.

The TRITON module and the v7-238-energy-group library cross sections of the ENDF/B-VII library for 1000 generations and 5000 neutrons per generation package was used for the burnup. It was assumed an irradiation history with 3 cycles of 420 days and 38.09 MW/MTU density power was assumed [24]. The temperatures used were 900 K for the fuels, 620 K for the cladding and 575 K for the moderator [24]. The reactor operates with 600 ppm borated water [24] and the results were compared with those obtained for the UO_2 fuel.

In order to preserve maximum accuracy during the depletion calculation, for the (Th-U)O_2 fuels, as well as, for (TRU-Th)O_2 and (TRU-U)O_2 fuels, the legacy addnux value of 3 has been included. TRITON allows the user to determine the set of nuclides added to the combustible material by means of control parameter parm = (addnux = N), where N is an integer $0 \leq N \leq 3$. In N = 3, 166 nuclides are added, deeming 232 nuclides and allowing a more detailed configuration. At high burnup levels, these nuclides have a small effect on the neutron spectrum of the system but generally contribute to the overall reactivity of the system. The k_{inf} evolution for all the fuels as a function of burnup are shown in Figure 11. Table 16 represents the k_{inf} for the different fuels in the begin of life (BOL) and in the end of cycle 3 (EOC3).

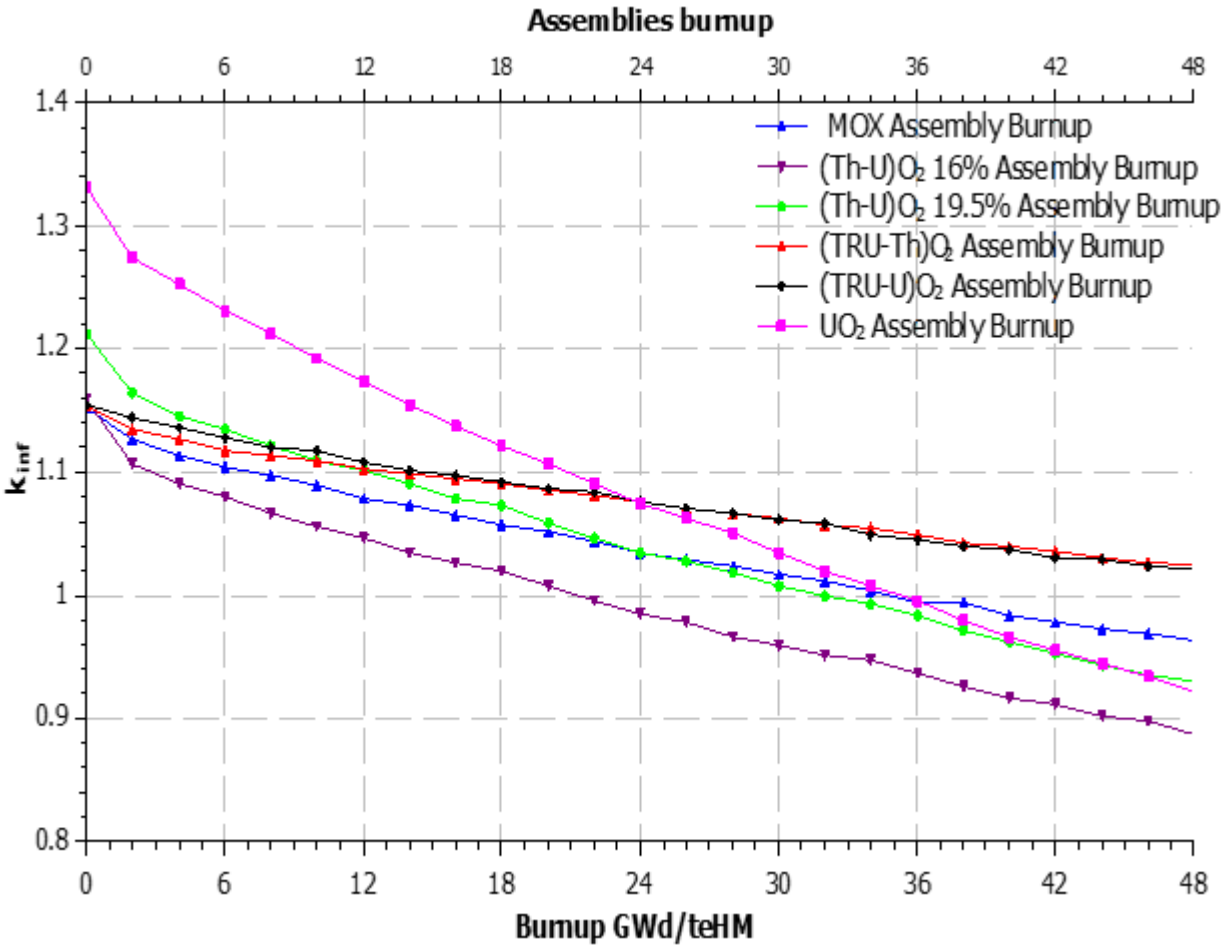

Figure 11 - k_{inf} evolution as function of burnup for UO_2, MOX, (Th-U)O_2-16%, (Th-U)O_2-19.5%, (TRU-Th)O_2 and (TRU-U)O_2 assemblies.

Table 16 – k_{inf} for all the different fuels in the begin of life (BOL) and in the end of cycle 3 (EOC3)

Fuel	**Initial k_{inf} (BOL)**	**Final k_{inf} (EOC 3)**
MOX	1.1517 ± 0.0033	0.9628
UO_2	1.3234 ± 0.0018	0.9216
(Th-U)O_2-19.5%	1.2147 ± 0.0012	0.9293
(Th-U)O_2-16%	1.1587 ± 0.0026	0.8872
(TRU-Th)O_2	1.1525 ± 0.0010	1.0255
(TRU-U)O_2	1.1553 ± 0.0011	1.0205

The reactivity of the nuclear fuels decreases with irradiation in different proportion due to the transformation of heavy nuclides and the formation of fission products [24]. The UO_2 fuel has a significant ^{238}U and ^{235}U concentration. In the ^{238}U and ^{235}U decay chains there are no other fissile isotopes which explain the prompt decrease in the UO_2 fuel curve. The (Th-U)O_2-19.5% and (Th-U)O_2-16% fuels have a high concentration of fertile ^{232}Th isotope, which consequently increase the ^{233}U production. These fuels also have a considerable concentration of ^{238}U and ^{235}U, which do not rise the amount of new fissile materials. Thus, it is ensured that (Th-U)O_2-19.5% and (Th-U)O_2-16% fuels have curves with a steep slope, but not as much as the UO_2 fuel curve. The (TRU-Th)O_2 fuel has a large amount of the fertile ^{232}Th isotope in its composition. This isotope, which is a neutron absorber capable of being transformed into the fissile isotope ^{233}U by neutron capture. MOX fuel is a low enriched uranium (LEU) fuel with only 0.25 w/o ^{235}U and 5.136 w/o fissile material [24]. The presence of fissile material such as the ^{239}Pu in MOX fuel makes possible to maintain the chain reaction, ensuring a smooth curve for this fuel. Again in (TRU-U)O_2 fuel the fissile ^{239}Pu isotope ensure the fission reactions for longer periods. The investigation of the reprocessed transuranic fuels showed that the infinite multiplication factor has a slower reduction when compared to UO_2 fuel, suggesting the possibility of burnup extension.

The focus of the present study is to evaluate the fuel depletion in the spent fuel pool (SFP). Therefore, the safety parameters such as radioactivity, decay heat, ingestion and inhalation radiotoxicity as well as the criticality into the spent fuel pool will be analyzed in the following sessions. The fuel assemblies are inserted in the spent fuel pool after the reactor shutdown. Tables 17 and 18 present the fuel compositions when the assemblies are inserted in the SFP.

Table 17 – MOX, (Th-U)O_2-19.5% and (Th-U)O_2-16% fuel compositions after EOC 3

atom/barn.cm			
Nuclide	**MOX**	**(Th-U)O_2-19.5%**	**(Th-U)O_2-16%**
^{232}U	6.9299E-10	5.05406E-05	5.43208E-05
^{233}U	9.4437E-10	1.05255E-02	1.06788E-02
^{234}U	3.8957E-05	1.64900E-03	1.86137E-03
^{235}U	1.0174E-03	1.03366E-02	6.76176E-03
^{236}U	2.3948E-04	5.77555E-03	4.89589E-03
^{237}U	1.5658E-06	6.39809E-06	6.61241E-06
^{238}U	7.9961E-01	6.49885E-01	1.77770E-01
^{238}Pu	1.4892E-03	1.89640E-04	1.93064E-04
^{239}Pu	2.0186E-02	2.01695E-03	1.93874E-03
^{240}Pu	1.6344E-02	7.00263E-04	7.28895E-04
^{241}Pu	9.1731E-03	6.53213E-04	6.57283E-04
^{242}Pu	6.0207E-03	2.83740E-04	3.41776E-04
^{232}Th	1.3881E-10	6.49885E-01	6.47387E-01
^{230}Th	1.1650E-10	6.90907E-07	7.60742E-07
^{241}Am	7.6741E-04	2.38849E-05	2.29410E-05
^{242m}Am	2.1801E-05	5.33744E-07	5.02903E-07
^{243}Am	1.6335E-03	7.30671E-05	9.41032E-05
^{235}Np	8.1074E-14	1.68834E-13	1.0772E-13
^{236}Np	1.2263E-11	1.46925E-11	1.3147E-11
^{237}Np	1.6867E-04	5.42020E-04	5.07132E-04
^{238}Np	1.2583E-07	4.05908E-07	5.56612E-07
^{239}Np	2.9206E-05	9.23009E-06	1.31798E-05
^{241}Cm	3.6402E-11	3.8437E-14	1.3410E-14
^{242}Cm	3.5514E-05	1.8492E-07	2.0475E-07
^{243}Cm	1.2838E-06	4.6612E-09	5.4953E-09
^{244}Cm	2.4039E-05	5.524E-07	7.95125E-07
^{245}Cm	3.0271E-06	3.9916E-08	5.62711E-08

Table 18 – $(TRU\text{-}Th)O_2$, $(TRU\text{-}U)O_2$ and UO_2 fuel compositions after EOC 3

atom/barn.cm			
Nuclídeo	**$(TRU\text{-}Th)O_2$**	**$(TRU\text{-}U)O_2$**	**UO_2**
^{232}U	4.44834E-05	3.05700E-08	8.43001E-10
^{233}U	1.22924E-02	3.93874E-07	3.68479E-09
^{234}U	9.31845E-04	1.21807E-02	1.56940E-04
^{235}U	1.43562E-04	3.14336E-03	7.98596E-03
^{236}U	1.62667E-05	6.81213E-02	5.43919E-03
^{237}U	2.15568E-09	2.71521E-07	8.56986E-06
^{238}U	5.90829E-08	6.20854E-02	8.3208E-01
^{238}Pu	5.36487E-03	6.80485E-03	2.66048E-04
^{239}Pu	3.41556E-02	6.57215E-02	5.81913E-03
^{240}Pu	2.84600E-02	3.79512E-02	2.57114E-03
^{241}Pu	1.50050E-02	1.85256E-02	1.60098E-03
^{242}Pu	9.73300E-02	1.16081E-02	6.91202E-04
^{232}Th	7.37725E-01	7.13482E-09	3.59635E-10
^{230}Th	1.54016E-06	1.09172E-07	1.48186E-09
^{241}Am	3.89590E-03	5.76676E-03	5.51771E-05
^{242m}Am	1.82944E-04	2.60886E-04	1.19668E-06
^{243}Am	2.90098E-03	3.27789E-03	1.78509E-04
^{235}Np	2.99744E-10	2.49342E-10	2.36803E-11
^{236}Np	7.08658E-09	3.63422E-08	2.14035E-09
^{237}Np	2.77481E-03	7.54661E-03	6.31639E-04
^{238}Np	1.40408E-06	3.05973E-06	7.45441E-07
^{239}Np	3.45522E-09	1.95710E-05	3.67396E-05
^{241}Cm	1.3203E-11	5.23954E-11	3.84326E-11
^{242}Cm	4.54297E-04	4.70504E-04	4.99725E-07
^{243}Cm	7.29721E-05	2.64522E-05	1.35261E-08
^{244}Cm	1.88622E-04	5.13152E-04	1.82098E-06
^{245}Cm	8.62136E-05	2.88156E-04	1.34681E-07

After irradiation, all fuel assemblies shall be conveyed to a spent fuel pool. For criticality accident requirements, the k_{inf} of the spent fuel storage racks loaded with fuel of the maximum fuel assembly reactivity must not exceed 0.95, if flooded with unborated water [28,29]. The decay heat, radioactivity, as well as, inhalation and ingestion radiotoxicity analysis will be also discussed subsequently in this study.

5. SPENT FUEL POOL

The pool model used in this study was based on the cooling pool described in the Angra 2, Final Safety Analysis Report - FSAR [28]. The pool's dimension are 15.914 x 5.668 m and 11.6568 m depth. The pitch distance in the spent fuel pool was studied by adjusting the maximum possible number of elements that maintain the pool in a subcriticality state.

The criticality safety analysis considers the minimum boron concentration of 2300 ppm specified in FSAR and required for SFP [28]. Figure 12 illustrates the SFP modeled loaded at its entirely capacity.

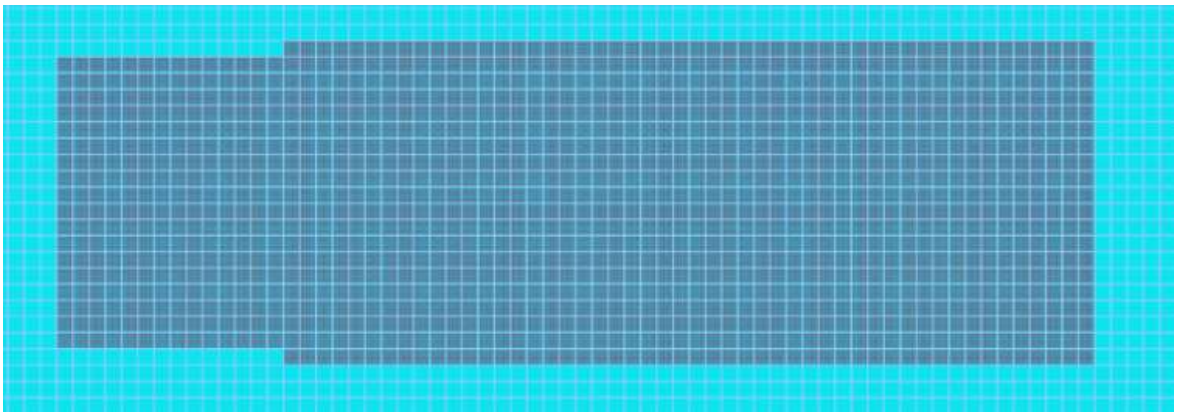

Figure 12 - Spent Fuel Pool using Angra 2 FSAR as a model [28].

The fuels assemblies are arranged in the storage racks in such a way to ensure the deep subcriticality of the SFP. The authorized are expected to put spent fuel assemblies into the storage following the 1×4 and 1×3 repeating pattern or equivalent [30,31]. It was required to find the minimum pitch distance that would optimize the elements arrangement in the SFP keeping the system under the upper criticality limit [28].

Aiming to make a close analysis of the nuclear power plants and to ensure a safety project, three different load patterns were designed for assemblies while they are into the spent fuel pool. In a first moment, a uniform configuration was adopted placing only one type of fuel in the SFP. In a second instance, a mixed pattern is considered in which the standard UO_2 fuel assemblies are placed in the SFP together with reprocessed and thorium-based fuel assemblies. The mixed pool is first

filled with one MOX, (Th-U)O_2, (TRU-Th)O_2 or (TRU-U)O_2 fuel assembly per each three standard UO_2 fuel assemblies, following the ratio 1:3 assemblies, respectively. Thereafter, one MOX, (Th-U)O_2, (TRU-Th)O_2 or (TRU-U)O_2 fuel assembly per each two standard UO_2 fuel assemblies were placed into the mixed spent fuel pool, taking into consideration 1:2 ratio, respectively. Figures 13 and 14 show the two load patterns for the mixed pool model containing one MOX or (Th-U)O_2 or (TRU-Th)O_2 or (TRU-U)O_2 fuel assembly together with three and two UO_2 fuel assemblies, respectively.

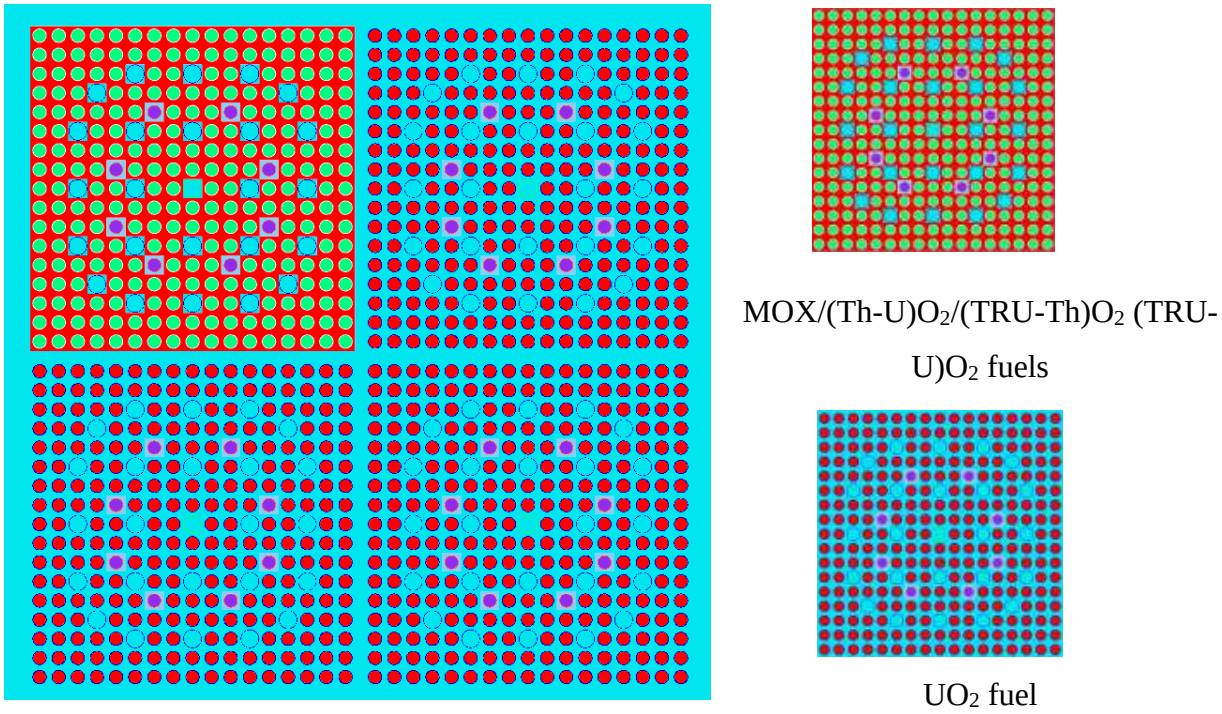

Figure 13 – The mixed pool model considering 1/4 of MOX/(Th-U)O_2/(TRU-Th)O_2/(TRU-U)O_2 assembly placed with 3/4 of UO_2 fuel assemblies [author].

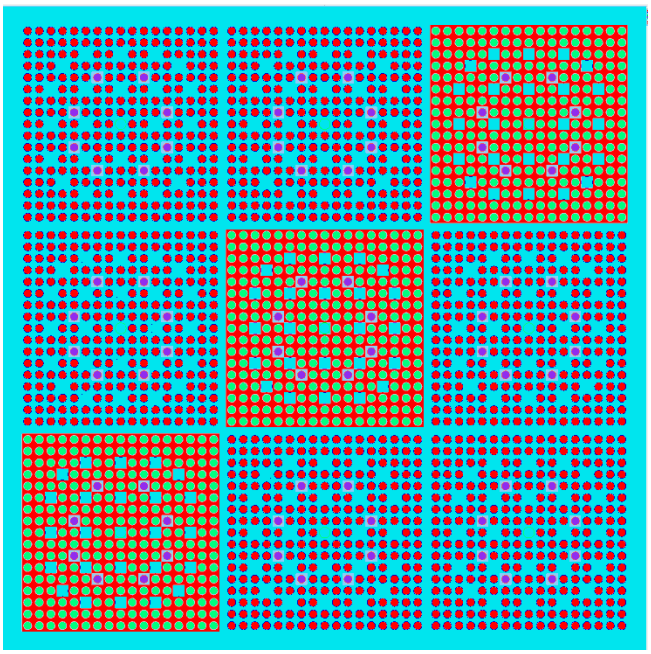

Figure 14 – The mixed pool model considering 1/3 of MOX/(Th-U)O_2/(TRU-Th)O_2/(TRU-U)O_2 fuel assembly placed with 2/3 of UO_2 fuel assemblies[author]

To be conservative, the parameters in the single spent fuel pool as well as in the mixed spent fuel pool were simulated at 298 K, once that at this temperature would be expected the higher multiplication factor possible due to the Doppler Effect.

5.1. CRITICALITY IN SPENT FUEL POOL

The safe criticality required for the single and the mixed spend fuel pool was obtained for UO_2, MOX, (Th-U)O_2-19.5%, (Th-U)O_2-16%, (TRU-Th)O_2 and (TRU-U)O_2 fuels in SCALE 6.0 code via KENO-VI sequence and CSAS6 module with v7-238-energy-group library using 2000 generations and 2000 neutrons per generation. The fuel assemblies were inserted in the spent fuel pool. 1252 assemblies were inserted altogether, and this number was attained considering the upper multiplication factor limit of 0.95, following the Final Safety Analysis Report [28] and the NRC regulation 10 CFR 50.68 [29]. In the 1/4 mixed pool, 313 MOX/(Th-U)O_2-19.5%/(Th-U)O_2-16%/(TRU-Th)O_2/(TRU-U)O_2 assemblies were placed together with 939 UO_2 assemblies while in

the 1/3 mixed pool, 418 MOX/(Th-U)O_2-19.5%/(Th-U)O_2-16%/(TRU-Th)O_2/(TRU-U)O_2 assemblies were placed together with 834 UO_2 assemblies.

The minimum pitch distance search was obtained by KENO-V sequence and CSAS5-S module in the SCALE 6.0 code. It was verified that a 0.695 cm pitch distance would maintain the criticality under the upper criticality limit of 0.95 and assure the maximum elements capacity in the SFP. Tables 19 to 21 show the k_{inf} for the fuels inserted in the single and mixed spent fuel considering different load patterns.

Table 19 – Fuels initial k_{inf} for the spent fuel pool using the single load pattern

Fuel	**k_{inf}**
MOX	0.84409 ± 0.00032
(Th-U)O_2-19.5%	0.68867 ± 0.00021
(Th-U)O_2-16%	0.64962 ± 0.00022
(TRU-Th)O_2	0.93698 ± 0.00028
(TRU-U)O_2	0.95068 ± 0.00025
UO_2	0.78256 ± 0.00029

Table 20 – Fuels initial k_{inf} for the mixed spent fuel pool using the 1/4 load patterns

$^1/_4$ mixed load pattern	**k_{inf}**
$^1/_4$ of MOX	0.80690 ± 0.00027
$^1/_4$ of (Th-U)O_2-19.5%	0.76503 ± 0.00021
$^1/_4$ of (Th-U)O_2-16%	0.75407 ± 0.00023
$^1/_4$ of (TRU-Th)O_2	0.84213 ± 0.00026
$^1/_4$ of (TRU-U)O_2	0.85788 ± 0.00030

Table 21 – Fuels initial k_{inf} for the mixed spent fuel pool using the 1/3 load pattern

$^1/_3$ mixed load pattern	**k_{inf}**
$^1/_3$ of MOX	0.82245 ± 0.00027
$^1/_3$ of (Th-U)O_2-19.5%	0.76663 ± 0.00024
$^1/_3$ of (Th-U)O_2-16%	0.75328 ± 0.00022
$^1/_3$ of (TRU-Th)O_2	0.86564 ± 0.00029
$^1/_3$ of (TRU-U)O_2	0.87183 ± 0.00027

The infinite multiplication factor values showed in Tables 19 to 21 are in accordance with the curves plotted in Figure 11, once that follow the same k_{inf} descending order.

Filling the standard UO_2 assemblies into the mixed spent fuel pool together with MOX, (TRU-Th)O_2 or (TRU-U)O_2 fuel assemblies made the criticality decrease. Even though criticality has increased when UO_2 fuel assemblies were inserted along with (Th-U)O_2-19.5% and (Th-U)O_2-16% fuel assemblies in the pool, for all the two mixed load models, the $k_{safe} \leq 0.95$ requirement for the Spent Fuel Pool remains guaranteed as established by Angra 2 - Final Safety Analysis Report and the NRC regulation 10 CFR 50.68 [28,29].

The decay heat, radioactivity, as well as inhalation and ingestion radiotoxicity for all fuels were performed over 50 years in the SFP and in the mixed pool using TRITON sequences making use of T6-DEPL module and v7-238-energy-group library, including bias and uncertainty parameter.

5.2. DECAY HEAT

Figure 15 shows the decay heat considering the insertion of all fuel assemblies in the SFP over 50 years. Figures 16 and 17 show the decay heat curves when different proportions of UO_2 are inserted together with MOX, (Th-U)O_2 16%, (Th-U)O_2 19.5%, (TRU-Th)O_2 or (TRU-U)O_2 in the mixed pool. It is shown that the reprocessed thorium-transuranic and the uranium-transuranic fuels have

the highest decay heat values when they are inserted alone or together with UO_2 fuel. The high decay heat for these fuels is due to the high amount of alpha emitters such as ^{239}Pu, ^{240}Pu and ^{241}Pu. Table 22, 24 and 25 show the initial decay heat values, when the fuel assemblies are loaded in the single pool, 1/4 mixed pool and 1/3 mixed pool as well as the final decay heat values, after 50 years.

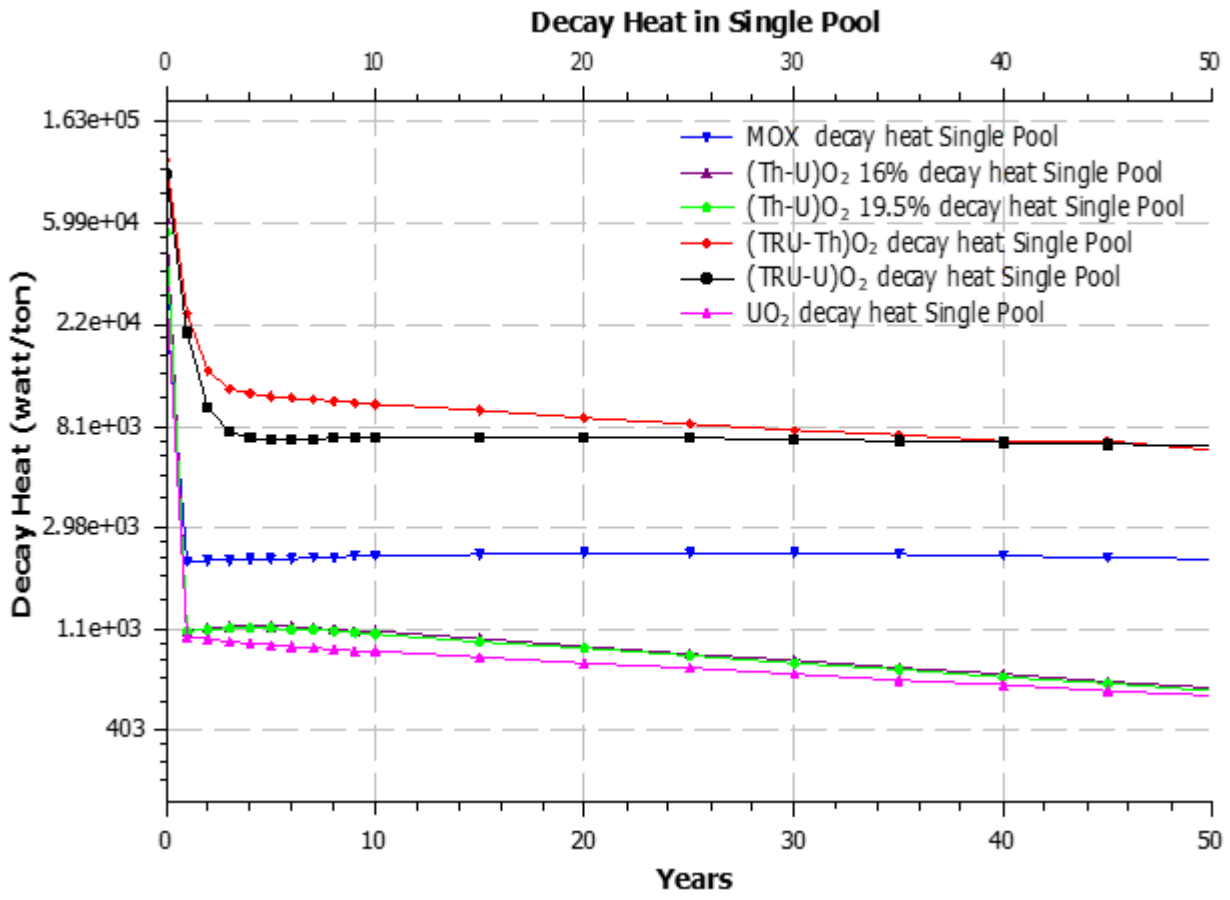

Figure 15 – Decay Heat curves for UO_2, MOX, (Th-U)O_2-16%, (Th-U)O_2-19.5%, (TRU-Th)O_2 and (TRU-U)O_2 assemblies in the SFP.

Table 22 – Initial and final fuel assemblies decay heat in the single pool model

	Initial decay heat in the single pool (watt/ton)	**Final decay heat in the single pool (watt/ton)**
UO_2	31,720	573.4
MOX	25,770	2,203
(Th-U)O_2-16%,	62,810	620.3
(Th-U)O_2-19.5%,	54,950	603.6
(TRU-Th)O_2	111,400	6,406
(TRU-U)O_2	96,890	6,735

Among the actinides, the plutonium isotopes are the ones that, initially, contribute the most to the decay heat of irradiated fuels in the PWR reactor. Table 23 represents the amount of ^{239}Pu, ^{240}Pu and ^{241}Pu in all fuels 3 days after the reactor shutdown, whe the fuel assemblies are loaded in the spent fuel pool.

Table 23 – Amount of ^{239}Pu, ^{240}Pu and ^{241}Pu in fuel composition when inserted in the single SFP

	^{239}Pu	**^{240}Pu**	**^{241}Pu**
UO_2	5.81913E-03	2.57114E-03	1.60098E-03
MOX	2.01863E-02	1.63439E-02	9.17314E-03
(Th-U)O_2-16%,	1.93874E-03	7.28895E-04	6.57283E-04
(Th-U)O_2-19.5%,	2.01695E-03	7.00263E-04	6.53213E-04
(TRU-Th)O_2	3.41556E-02	2.84600E-02	1.50050E-02
(TRU-U)O_2	6.57214E-02	3.79512E-02	1.85256E-02

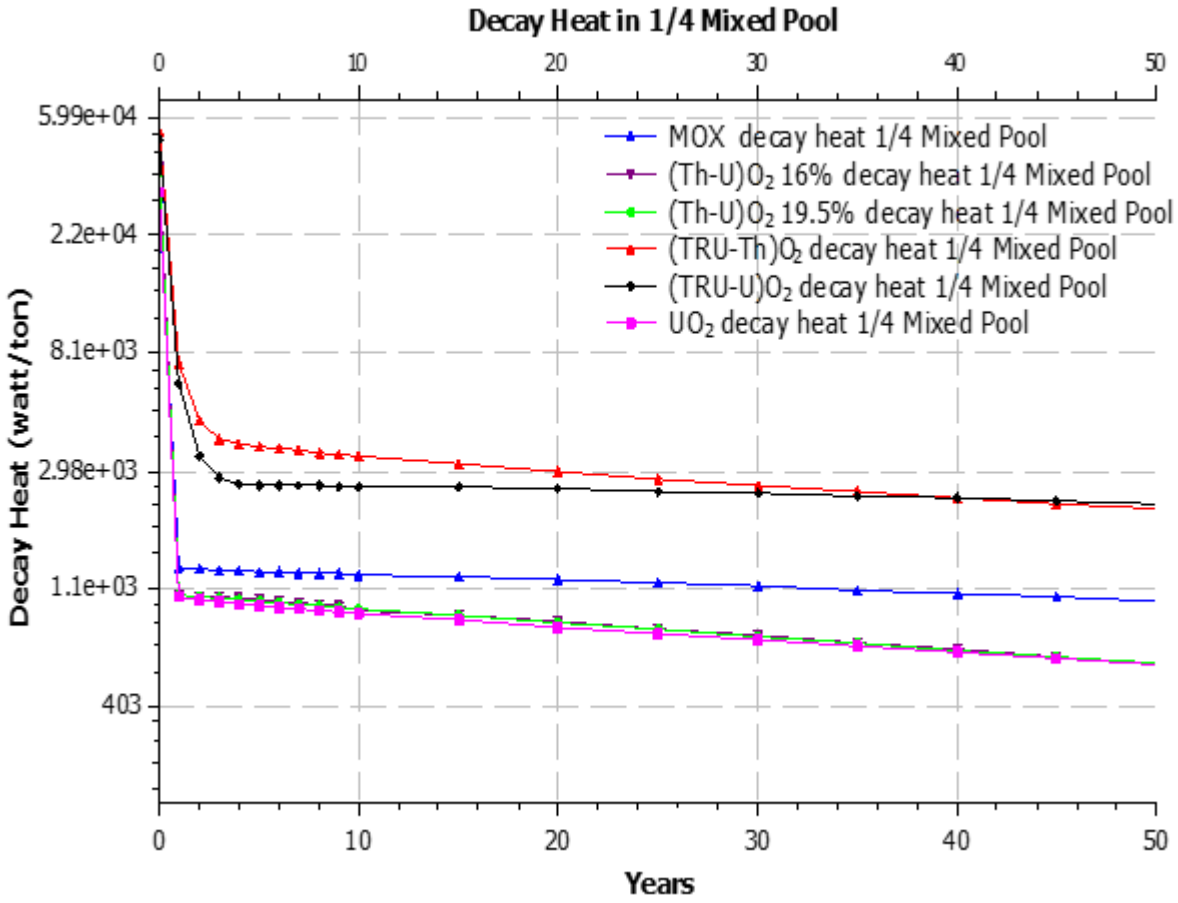

Figure 16 – Decay heat curves for the 3/4 UO_2 mixed pool combined with 1/4 of MOX, (Th-U)O_2-16%, (Th-U)O_2-19.5%, (TRU-Th)O_2 and (TRU-U)O_2 in the SFP.

Table 24 – Initial and final fuel assemblies decay heat for the 1/4 mixed pool

	Initial decay heat in the 1/4 Mixed pool (watt/ton)	**Final decay heat in the 1/4 Mixed pool (watt/ton)**
UO_2	31,720	573.4
MOX	30,250	987.8
(Th-U)O_2-16%,	39,070	585.2
(Th-U)O_2-19.5%,	37,220	581.3
(TRU-Th)O_2	53,300	2,151
(TRU-U)O_2	49,470	2,248

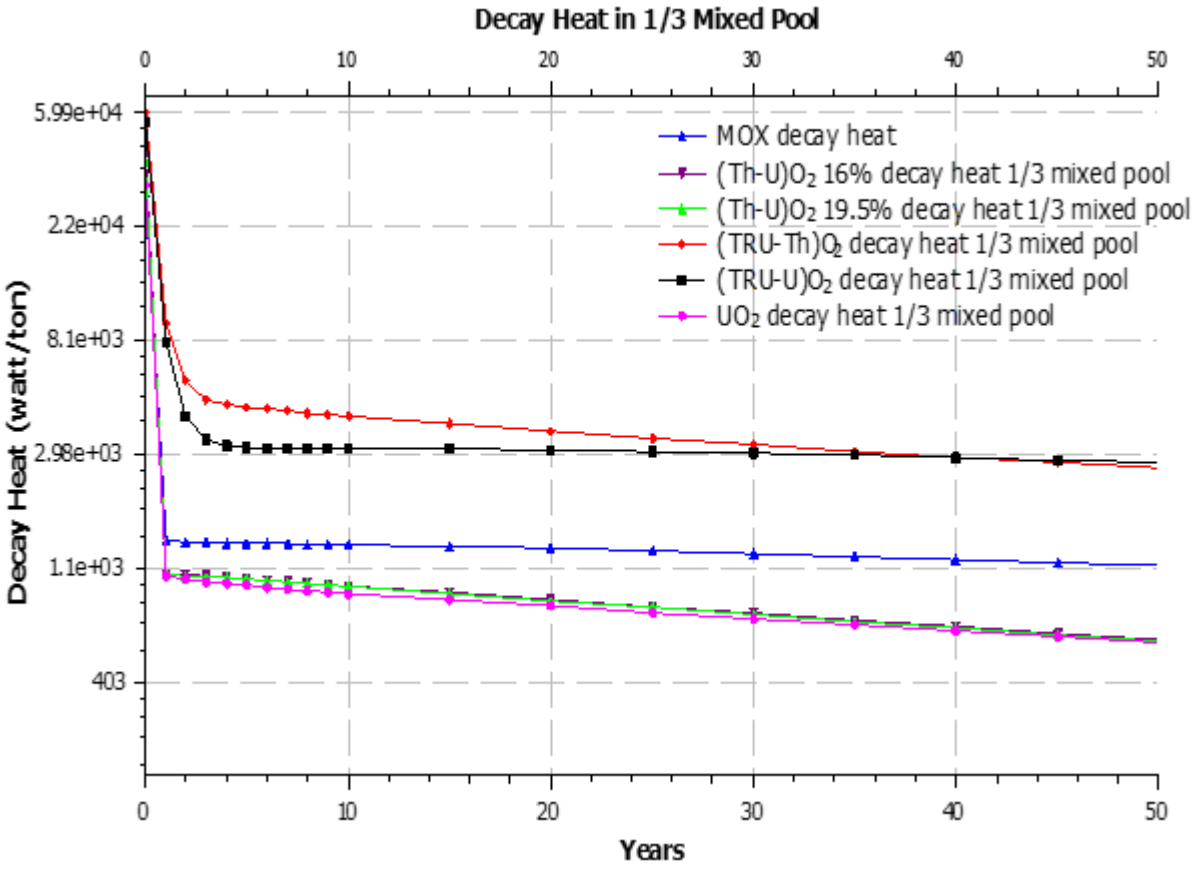

Figure 17 – Decay heat curves for the 2/3 UO_2 Mixed pool combined with 1/3 of MOX, (Th-U)O_2-16%, (Th-U)O_2-19.5%, (TRU-Th)O_2 and (TRU-U)O_2.

Table 25 – Initial and final fuel assemblies decay heat for the 1/3 mixed pool

	Initial decay heat in the 1/3 Mixed pool (watt/ton)	**Final decay heat in the 1/3 Mixed pool (watt/ton)**
UO_2	31,760	574.2
MOX	29,750	1,126
(Th-U)O_2-16%,	41,590	589
(Th-U)O_2-19.5%,	39,100	583.7
(TRU-Th)O_2	60,260	2,661
(TRU-U)O_2	55,170	2,788

Once that MOX, (TRU-Th)O_2 and (TRU-U)O_2 fuels assemblies are inserted in the mixed pool together with the standard UO_2 assemblies, a decrease in the decay heat values has been verified for these fuels, extending their use and making feasible the use of thorium-transuranic and uranium-transuranic fuels in the PWR core.

5.3. RADIOACTIVITY

The UO_2, (Th-U)O_2-16%, and (Th-U)O_2-19.5% fuels emit the least radioactivity while (TRU-Th)O_2 and (TRU-U)O_2 fuels emit the highest radioactivity. MOX fuel emits radioactivity with intermediate values. However, a closer look allows us to say that the radiation profile emitted by all the fuels into the spent fuel pool has a similar shape. The radioactivity decreases substantially within the first year, when the fuels are inserted in the spent fuel pool, and then show a gradual decrease over 50 years. The radioactivity for the six spent fuels in the SFP considering the assemblies in single pool and the different configurations in the mixed pool is plotted against time in Figures 18, 19 and 20. Tables 26, 27 and 28 represent the initial radioactivity values as well as radioactivity after 50 years for all the fuel assemblies considering the single pool, 1/4 mixed pool and 1/3 mixed pool load patterns.

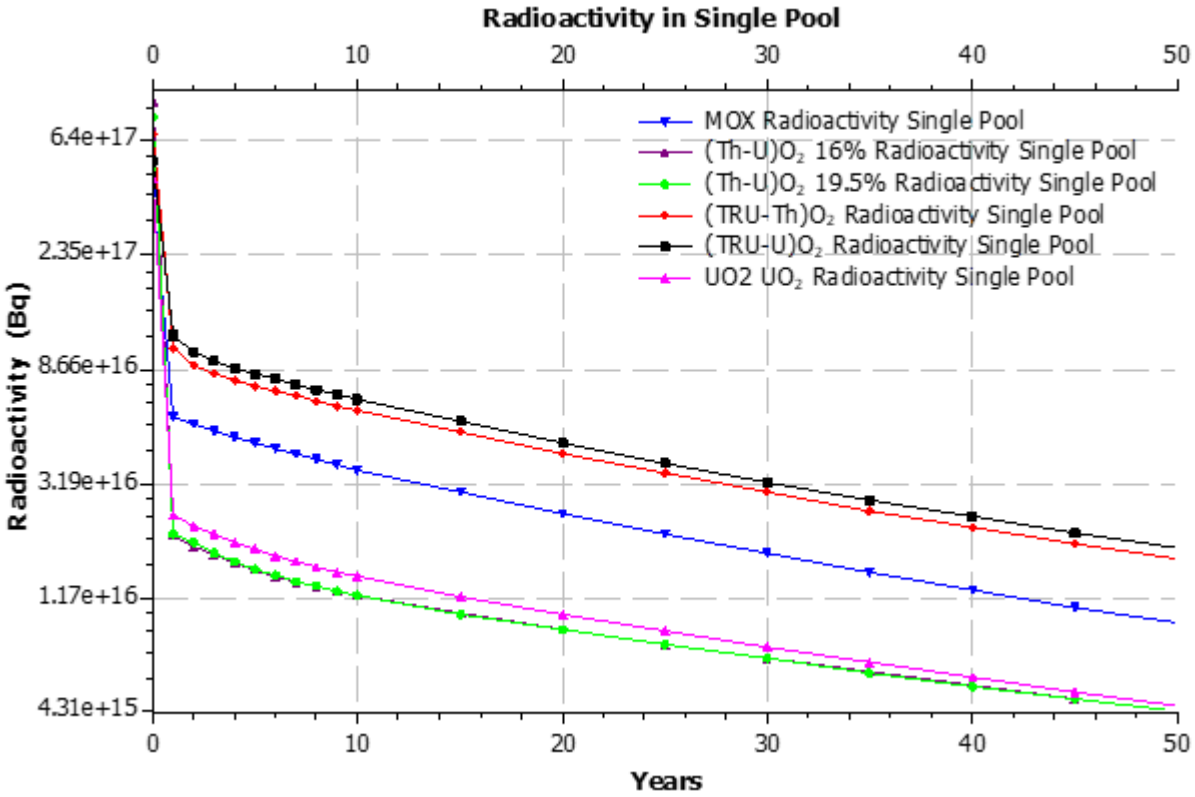

Figure 18 - Radioactivity curves for UO_2, MOX, (Th-U)O_2-16%, (Th-U)O_2-19.5%, (TRU-Th)O_2 and (TRU-U)O_2 assemblies in the SFP.

Table 26 – Initial and final fuel assemblies radioactivity for the single pool load pattern

	Initial radioactivity in the single pool (Bq)	**Final radioactivity in the single pool (Bq)**
UO_2	4.628e+17	4.538e+15
MOX	3.978e+17	9.361e+15
(Th-U)O_2-16%,	9.093e+17	4.311e+15
(Th-U)O_2-19.5%,	7.931e+17	4.283e+15
(TRU-Th)O_2	6.844e+17	1.649e+16
(TRU-U)O_2	5.369e+17	1.824e+16

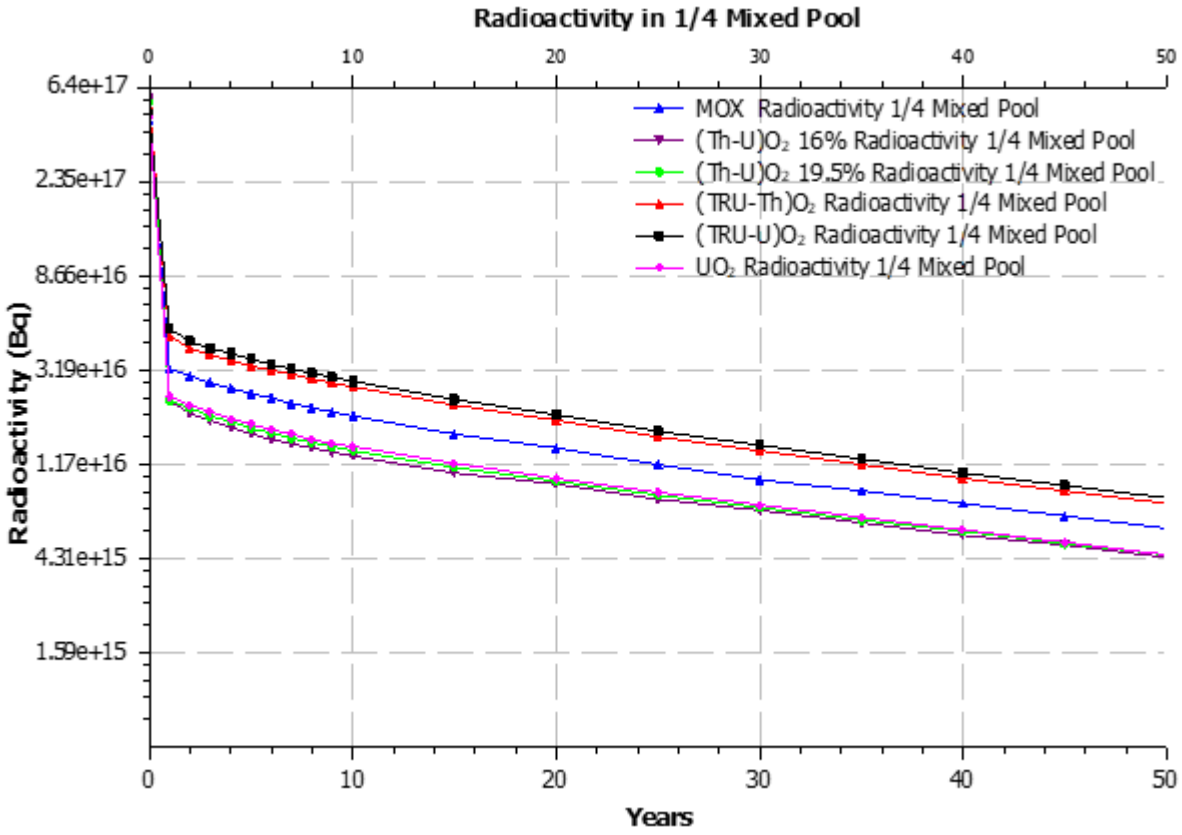

Figure 19 - Radioactivity curves for the 3/4 UO_2 Mixed pool combined with 1/4 MOX, (Th-U)O_2-16%, (Th-U)O_2-19.5%, (TRU-Th)O_2 and (TRU-U)O_2.

Table 27 – Initial and final fuel assemblies radioactivity for the 1/4 mixed pool load pattern

	Initial radioactivity in the 1/4 mixed pool (Bq)	**Final radioactivity in the 1/4 mixed pool (Bq)**
UO_2	4.628e+17	4.538e+15
MOX	4.469e+17	5.984e+15
(Th-U)O_2-16%,	5.684e+17	4.391e+15
(Th-U)O_2-19.5%,	5.41e+17	4.484e+15
(TRU-Th)O_2	5.233e+17	7.774e+15
(TRU-U)O_2	4.835e+17	8.266e+15

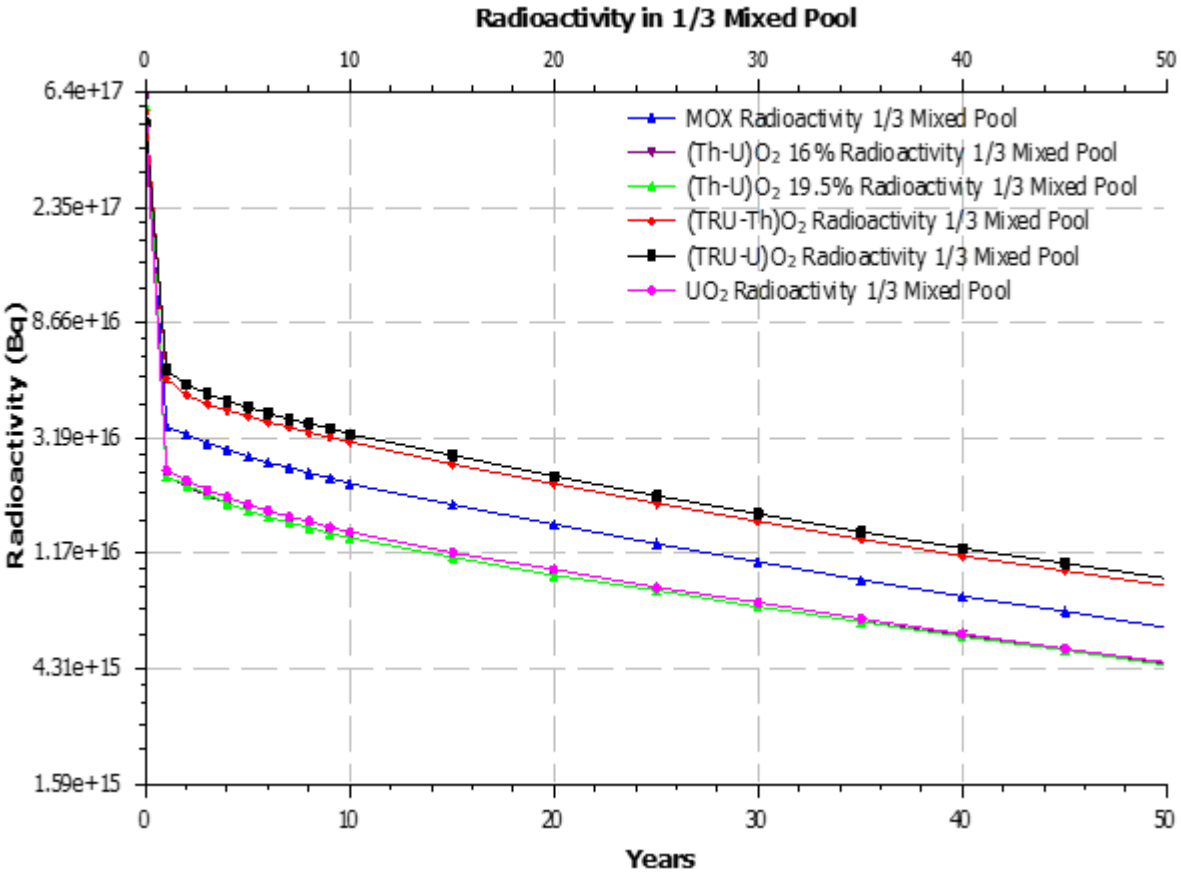

Figure 20 – Radioactivity curves for the 2/3 UO_2 Mixed pool combined with 1/3 MOX, (Th-U)O_2-16%, (Th-U)O_2-19.5%, (TRU-Th)O_2 and (TRU-U)O_2.

Table 28 – Initial and final fuel assemblies radioactivity for the 1/3 mixed pool load pattern

	Initial radioactivity in the 1/3 mixed pool (Bq)	**Final radioactivity in the 1/3 mixed pool (Bq)**
UO_2	4.634e+17	4.543e+15
MOX	4.414e+17	6.176e+15
(Th-U)O_2-16%,	6.045e+17	4.472e+15
(Th-U)O_2-19.5%,	5.678e+17	4.463e+15
(TRU-Th)O_2	5.426e+17	8.819e+15
(TRU-U)O_2	4.9e+17	9.467e+15

The fission products accounted for almost the entire radioactivity of spent fuel at the reactor shutdown and because of their short half-lives, the radioactivity levels decay quickly along 50 years. The more troublesome fission products from the waste management are ^{99}Tc and ^{129}I because of their long half-lives as well as ^{137}Cs, which are gamma emitter and so produce substantial decay heating. Table 29 summarizes the amount of ^{99}Tc, ^{129}I and ^{137}Cs in fuels composition 3 days after reactor shutdown.

Table 29 – Amount of ^{99}Tc, ^{129}I and ^{137}Cs in fuel compositions when fuel assemblies are inserted in the SFP

	^{99}Tc	**^{129}I**	**^{137}Cs**
UO_2	1.01618E-03	1.97461E-04	1.57932E-03
MOX	1.00210E-03	2.74382E-04	1.59201E-03
(Th-U)O_2-16%,	9.52727E-04	2.16905E-04	1.60947E-03
(Th-U)O_2-19.5%,	9.77886E-04	2.04933E-04	1.60582E-03
(TRU-Th)O_2	9.90423E-04	2.85141E-04	1.61225E-03
(TRU-U)O_2	1.08626E-03	2.81430E-04	1.60713E-03

5.4. INHALATION RADIOTOXICITY

Figures 21, 22 and 23 show the total inhalation radiotoxicity curves for the six fuels irradiated in the PWR system. The assemblies are again inserted in the spent fuel pool considering the single pool with just one type of fuel as well as the two different load pattern in the mixed pools. The (TRU-Th)O_2 and (TRU-U)O_2 fuel assemblies have the major inhaled radiotoxicity while the UO_2, (Th-U)O_2-16% and (Th-U)O_2-19.5% fuel assemblies have the least inhalaed radiotoxicity. MOX fuel emits inhaled radiotoxicity with intermediate values. Although the inhalation radiotoxicity profile emitted by the fuels is similar when inserted into both; single and mixed pools, the values are offset by several units when the (TRU-Th)O_2 and (TRU-U)O_2 fuel assemblies are mixed with the UO_2 fuel assemblies in the mixed pools.

Actinide contributions exceed fission product contributions to inhalation radiotoxicity The major actinides present in the fuels' composition dominate the inhaled radiotoxicity. For all the fuel cases, the isotopes of the plutonium element have a major contribution to the values of inhaled radiotoxicity, the ^{238}Pu, ^{239}Pu, ^{240}Pu, and ^{241}Pu isotopes are highlighted. Both thorium-based fuels and uranium-based fuel showed radiotoxicity values nearly equal. Tables 30, 31 and 32 represent the initial inhalation radiotoxicity values as well as the inhalation radiotoxicity after 50 years for all the fuel assemblies considering the single pool, 1/4 mixed pool and 1/3 mixed pool load patterns.

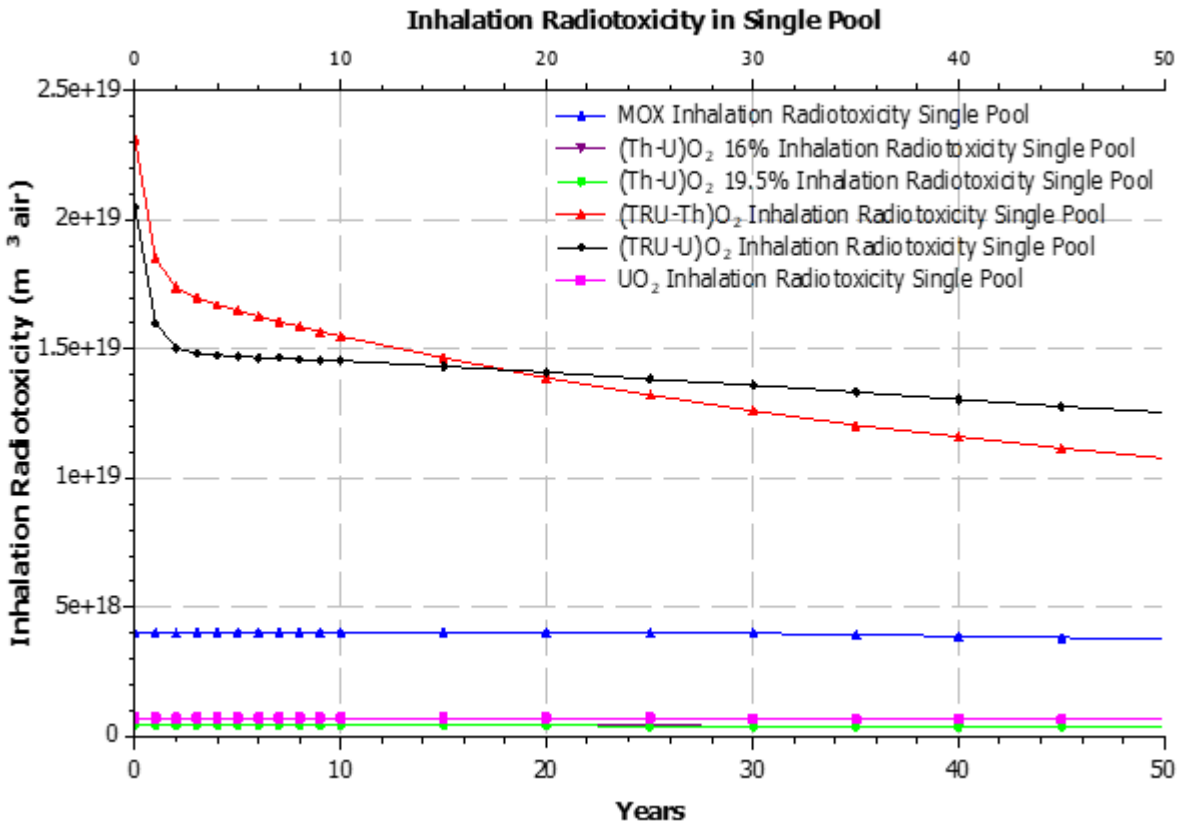

Figure 21 – Inhalation Radiotoxicity curves for UO_2, MOX, (Th-U)O_2-16%, (Th-U)O_2-19.5%, (TRU-Th)O_2 and (TRU-U)O_2 assemblies in the SFP.

Table 30 – Initial and final fuel assemblies inhalation radiotoxicity for the single pool load pattern.

	Initial inhalation radiotoxicity in the single pool (m^3 air)	**Final inhalation radiotoxicity in the single pool (m^3 air)**
UO_2	7.03e+17	6.535e+17
MOX	4.01e+18	3.784e+18
(Th-U)O_2-16%,	4.663e+17	3.763e+17
(Th-U)O_2-19.5%,	4.539e+17	3.694e+17
(TRU-Th)O_2	2.31e+19	1.076e+19
(TRU-U)O_2	2.048e+19	1.253e+19

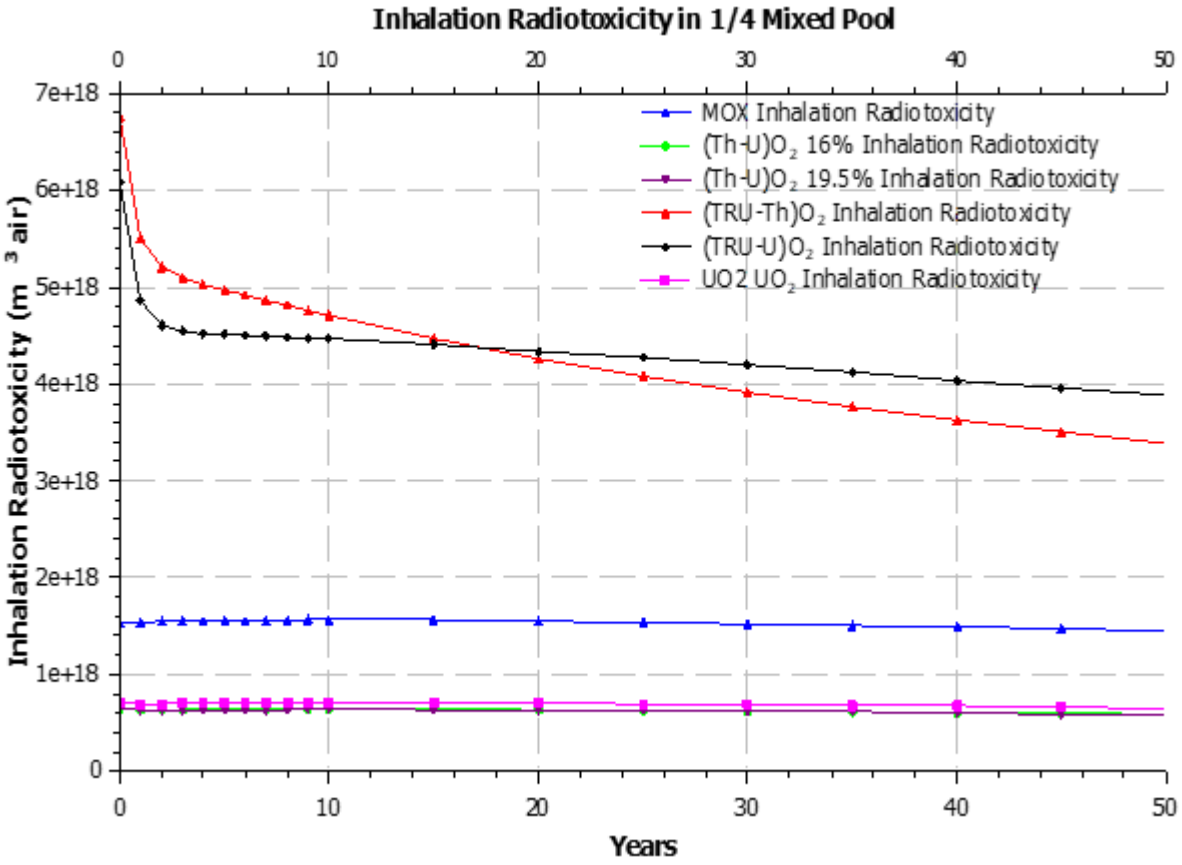

Figure 22 – Inhalation Radiotoxicity curves for the 1/4 UO_2 supercells combined with MOX, (Th-U)O_2-16%, (Th-U)O_2-19.5%, (TRU-Th)O_2 and (TRU-U)O_2 in the SFP

Table 31 – Initial and final fuel assemblies inhalation radiotoxicity for the 1/4 mixed pool load pattern.

	Initial inhalation radiotoxicity in the 1/4 mixed pool (m^3 air)	**Final inhalation radiotoxicity in the 1/4 mixed pool (m^3 air)**
UO_2	7.03e+17	6.535e+17
MOX	1.543e+18	1.449e+18
(Th-U)O_2-16%,	6.482e+17	5.826e+17
(Th-U)O_2-19.5%,	6.453e+17	5.876e+17
(TRU-Th)O_2	6.759e+18	3.387e+18
(TRU-U)O_2	6.077e+18	3.881e+18

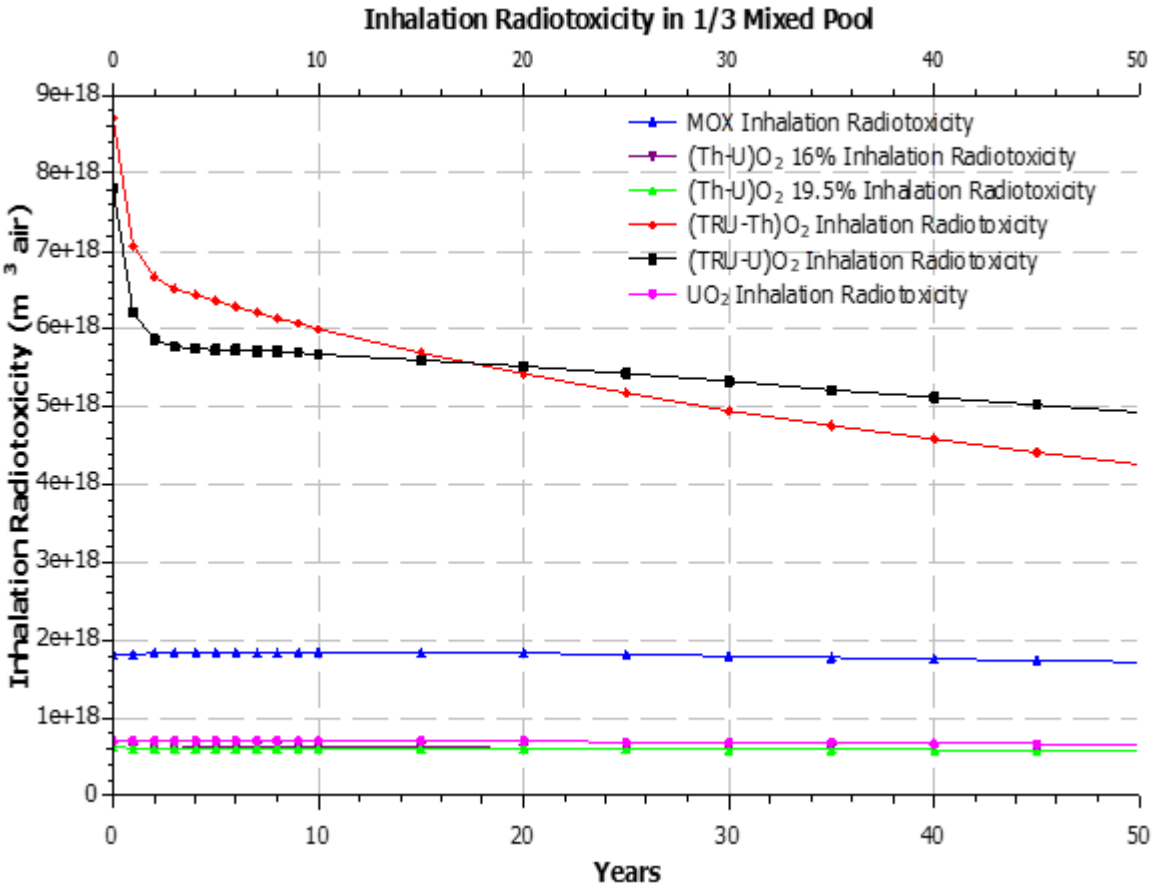

Figure 23 – Inhalation Radiotoxicity curves for the 2/3 UO_2 Mixed pool combined with 1/3 MOX, (Th-U)O_2-16%, (Th-U)O_2-19.5%, (TRU-Th)O_2 and (TRU-U)O_2

Table 32 – Initial and final fuel assemblies inhalation radiotoxicity for the 1/3 mixed pool load pattern

	Initial inhalation radiotoxicity in the 1/3 mixed pool (m^3 air)	**Final inhalation radiotoxicity in the 1/3 mixed pool (m^3 air)**
UO_2	7.038e+17	6.544e+17
MOX	1.823e+18	1.714e+18
(Th-U)O_2-16%,	6.291e+17	5.668e+17
(Th-U)O_2-19.5%,	6.252e+17	5.646e+17
(TRU-Th)O_2	8.716e+18	4.27e+18
(TRU-U)O_2	7.809e+18	4.921e+18

5.5. INGESTION RADIOTOXICITY

The ingested radiotoxicity for all fuel assemblies discharged from the PWR reactor and inserted into the single pool and into mixed pools is dominated by fission products over the 50 years. The (TRU-Th)O_2 and (TRU-U)O_2 fuels have the higest ingested radiotoxicity while the UO_2, (Th-U)O_2-16% and (Th-U)O_2-19.5% fuels have the least ingested radiotoxicity. MOX fuel emits ingested radiotoxicity with intermediate values. Although the ingestion radiotoxicity profile emitted by the fuels is similar when inserted into both; single and mixed pools, the values are offset by several units when the (TRU-Th)O_2 and (TRU-U)O_2 fuel assemblies are mixed with the UO_2 fuel assemblies in the mixed pools. Both thorium-based fuels and uranium-based fuel showed radiotoxicity values nearly equal and constant over the 50 years.

Figures 24, 25 and 26 show the total ingestion radiotoxicity curves for all the six fuel assemblies over to 50 years using different load patterns. Tables 33, 34 and 34 represent the initial ingesteion radiotoxicity values as well as the ingestion radiotoxicity after 50 years for all the fuel assemblies considering the single pool, 1/4 mixed pool and the 1/3 mixed pool load patterns.

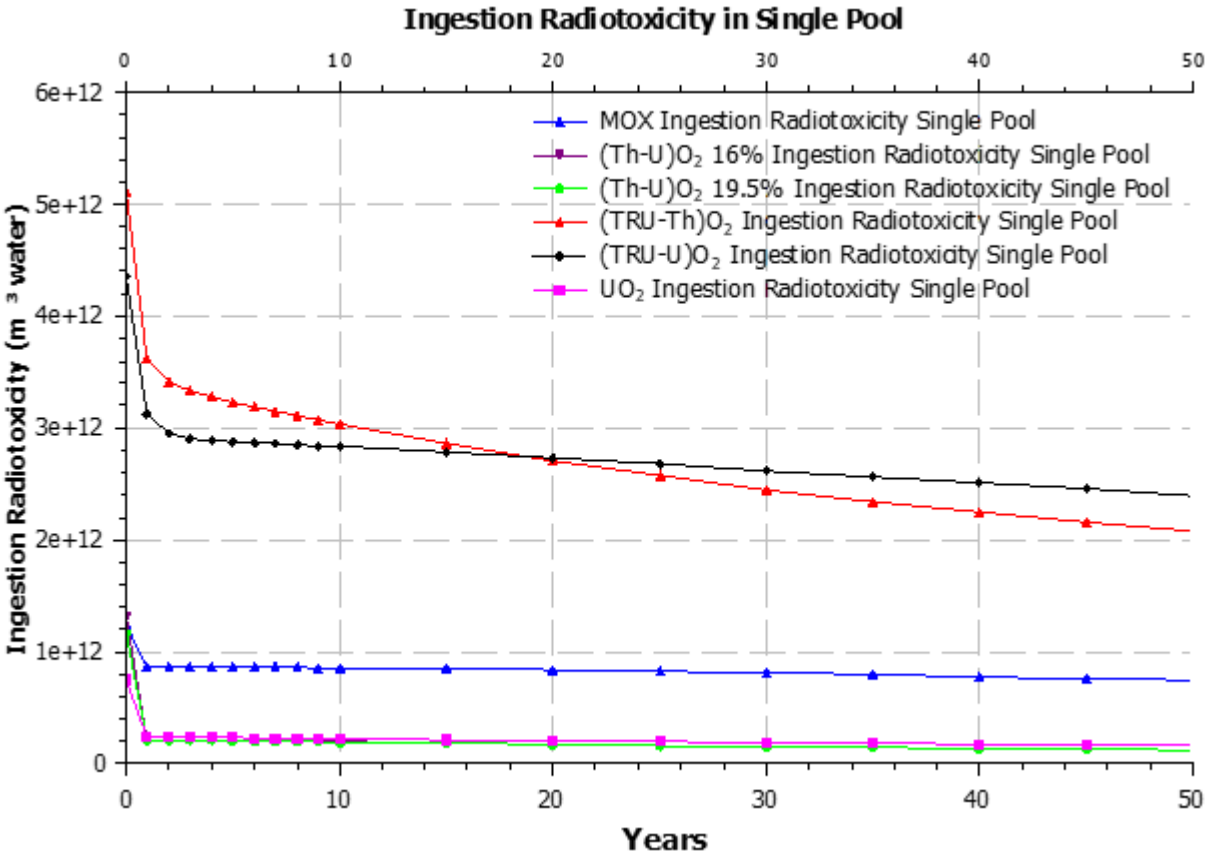

Figure 24 – Ingestion Radiotoxicity curves for UO_2, MOX, (Th-U)O_2-16%, (Th-U)O_2-19.5%, (TRU-Th)O_2 and (TRU-U)O_2 assemblies in the SFP

Table 33 – Initial and final fuel assemblies ingestion radiotoxicity for the single pool load pattern

	Initial ingestion radiotoxicity in the single pool (m^3 water)	**Final ingestion radiotoxicity in the single pool (m^3 water)**
UO_2	7.419E+12	1.575E+11
MOX	1.247E+12	7.476E+11
(Th-U)O_2-16%,	1.312E+12	1.200E+11
(Th-U)O_2-19.5%,	1.168E+12	1.176E+11
(TRU-Th)O_2	5.108E+12	2.077E+12
(TRU-U)O_2	4.355E+12	2.398E+12

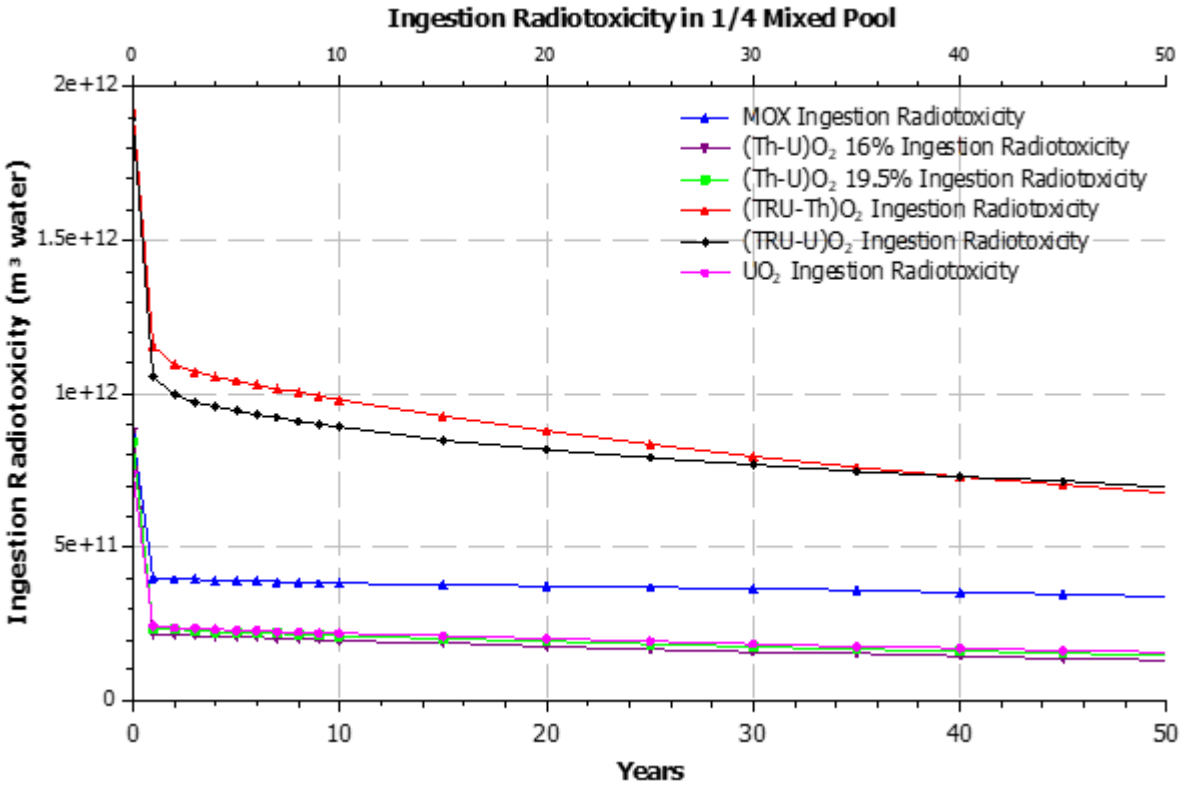

Figure 25 – Ingestion Radiotoxicity curves for the 1/4 UO_2 supercells combined with MOX, (Th-U)O_2-16%, (Th-U)O_2-19.5%, (TRU-Th)O_2 and (TRU-U)O_2 in the SFP

Table 34 – Initial and final fuel assemblies ingestion radiotoxicity for the 1/4 mixed pool load pattern

	Initial ingestion radiotoxicity in the 1/4 mixed pool (m^3 water)	**Final ingestion radiotoxicity in the 1/4 mixed pool (m^3 water)**
UO_2	7.419E+11	1.575E+11
MOX	8.705 E+11	3.371E+11
(Th-U)O_2-16%,	8.762E+11	1.314E+11
(Th-U)O_2-19.5%,	8.424E+11	1.483E+11
(TRU-Th)O_2	1.923E+12	6.766E+11
(TRU-U)O_2	1.893E+12	6.966E+11

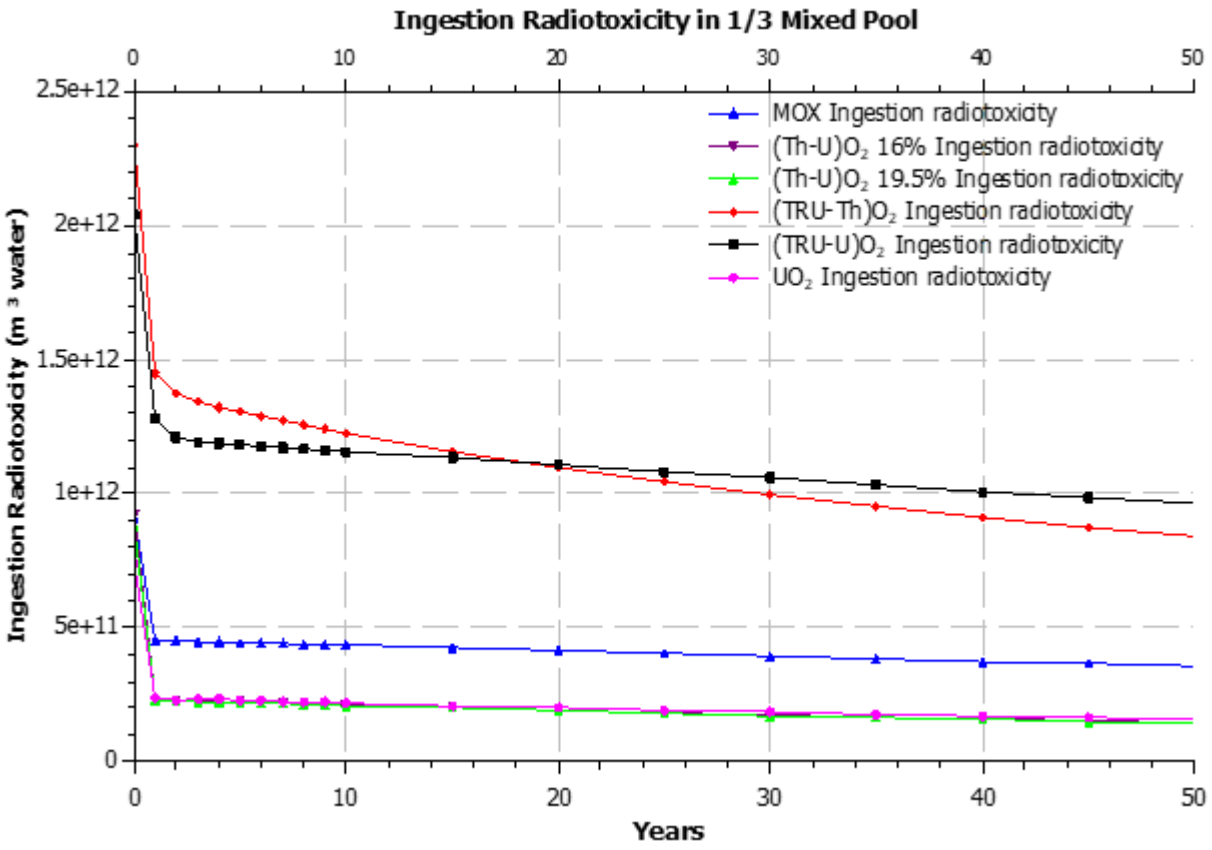

Figure 26 – Ingestion Radiotoxicity curves for the 2/3 UO_2 mixed pool combined with 1/3 MOX, (Th-U)O_2-16%, (Th-U)O_2-19.5%, (TRU-Th)O_2 and (TRU-U)O_2

Table 35 – Initial and final fuel assemblies ingestion radiotoxicity for the 1/3 mixed pool load pattern

	Initial ingestion radiotoxicity in the 1/3 mixed pool (m^3 water)	**Final ingestion radiotoxicity in the 1/3 mixed pool (m^3 water)**
UO_2	7.419E+11	1.577E+11
MOX	9.133E+11	3.574E+11
(Th-U)O_2-16%,	9.224E+11	1.458 E+11
(Th-U)O_2-19.5%,	8.769E+11	1.451 E+11
(TRU-Th)O_2	2.304E+12	8.443E+11
(TRU-U)O_2	2.041E+12	9.626E+11

6. SUPERCELL BENCHMARK DESCRIPTION

A supercell calculation for a MOX fuel element together with three UO_2 fuel assemblies was performed following again the Burn-up Credit Criticality Benchmark. Phase IV-B: Results and Analysis of MOX fuel Depletion Calculations [24] model. As show in figure 27, the supercell has a 34 x 34 geometry following the core model of a PWR reactor [24]. The model presents translational boundary conditions.

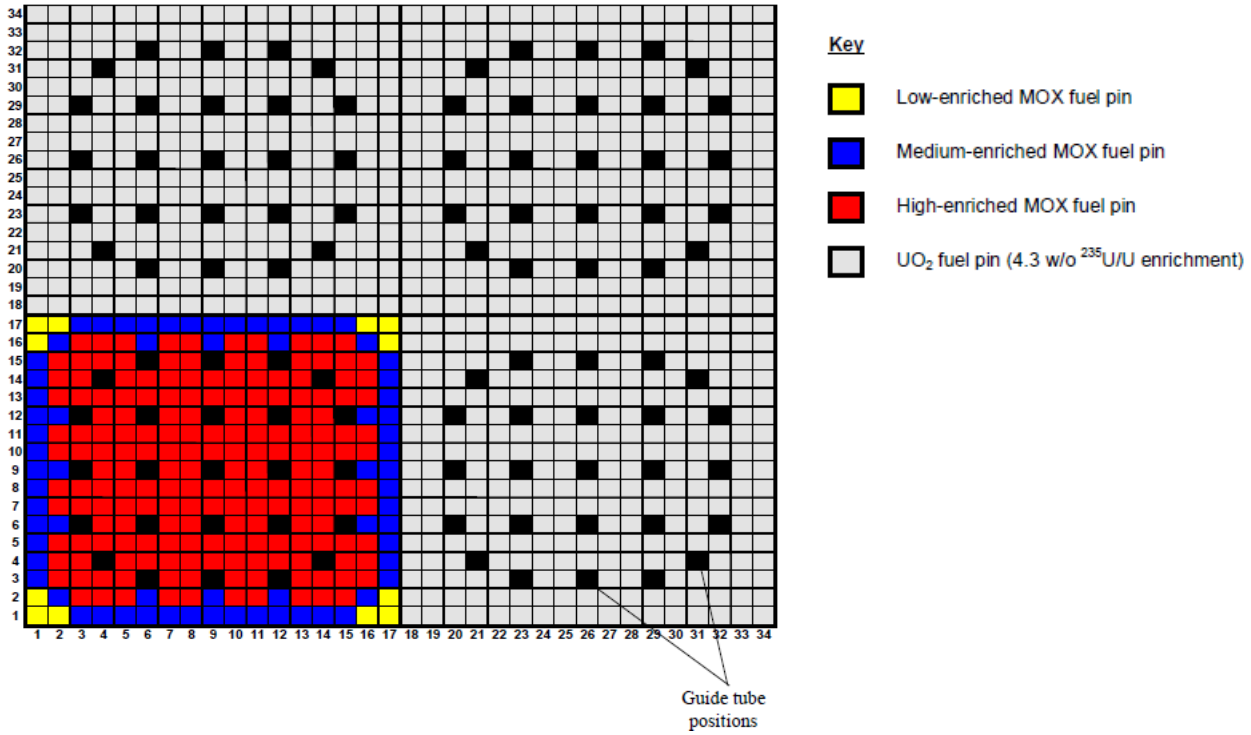

Figure 27 – MOX-UO_2 Supercell [24].

The MOX, (Th-U)O_2-16%, (Th-U)O_2-19.5%, (TRU-Th)O_2 and (TRU-U)O_2 fuel assemblies replaced one standard UO_2 fuel assembly in each 1/4 supercell. For the supercell calculations, the adjacent UO_2 fuel assemblies have an initial enrichment of 4.3 w/o ^{235}U/U and the power of the four-assembly cell should be set to attain the target burnup of the MOX assembly. Therefore, the same burnup target of 48 GWd/teHM were performed for the supercell model.

The adjacent MOX fuel has the same composition previously specified with three enrichment zones. The geometry data cover the simple MOX pin cell calculation, using the average MOX fuel

composition with pin cell geometry that conserves fuel-to-moderator ratio of the whole assembly in the previous calculation. The 96 guide tubes and instrumental tubes shall be also modelled as a water-filled reduced-density zircaloy tubes. The coolant and moderator are light water with 600 ppm boro.

6.1. SUPERCELL BENCHMARCK VALIDATION

The benchmark validation for MOX fuel supercell was performed using KENO-VI sequence making use of CSAS6 module in the SCALE6.0 code and ENDF/B-VII collapsed 238-energy-group library using the same irradiation history used in Phase IV-B benchmark. The MOX supercell benchmark results were compared with the results obtained at DEN/UFMG. The fuel supercell was modeled using the same geometry data and materials provided by the benchmark [24].

Table 36 summarizes the three operating cycles (EOC 1. EOC 2 and EOC 3) considering the values obtained for k_{inf} as well as Average, SD and RSD calculations for the eight groups that contributed for MOX supercell benchmark and DEN/UFMG value.

Table 36 – k_{inf} and reactivity change for the Supercell benchmark model including the participants and DEN/UFMG [24]

Participant		k_{inf}			Relative difference in k_{inf} (%)		
		EOC 1	EOC 2	EOC 3	EOC 1	EOC 2	EOC 3
NUPEC		1.09906	1.00024	0.92200	0.227	0.225	0.131
CEA		1.10154	1.00401	0.92554	0.475	0.602	0.223
GRS		1.09111	0.98840	0.91013	0.568	0.959	1.318
PSI		1.10163	1.00671	0.93077	0.484	0.872	0.746
BNFL		1.07571	0.98225	0.91344	2.108	1.574	0.987
JAERI		1.09525	0.99587	0.92144	0.154	0.212	0.187
DTLR		1.09880	0.99910	0.91980	0.201	0.111	0.351
ORNL		1.09382	0.99992	0.93210	0.297	0.193	0.879
DEN/UFMG		1.11420	1.00540	0.93460	1.741	0.742	1.129
Average	Before	1.09462	0.99706	0.92190			
	Updated	1.09679	0.99799	0.92331			
SD	Before	0.00849	0.00810	0.00766			
	Updated	0.00969	0.00761	0.00785			
RSD (%)	Before	0.78	0.81	0.83			
	Updated	0.88	0.76	0.85			

Table 36 presents the selected cases using different libraries to proceed with the validation jointly to the k_{inf} relative difference ($|k_{inf}$ Result - k_{inf} Average$|$). The results addressed as BEFORE do not consider the k_{inf} results from this work while the results referred to as UPDATED contemplate results from DEN/UFMG. Table 37 summarizes the participants with their analysis methods including neutron data code and library.

Table 37 – Benchmark participants and Supercell reactivity change analysis methods [24]

Participant	Institution	Neutron data processing Code	Neutron data Library
NUPEC	Nuclear Power Engineering Center	CASLIB	E4LBL70 based on ENDF/B-IV
CEA	CEA/DRN	NJOY from JEF-2 file	CEA-93 based on JEF-2.2 evaluations
GRS	Gesellschaft fur Anlagen und Reaktorsicherheit	RESMOD/HAMMER	292-group library JEF-2.2
PSI	Paul Scherrer Institute	BOXER	JEF-1
BNFL	British Nuclear Fuels Ltd	WIMS8A – NJOY & WILT	172-group
JAERI	Japan Atomic Energy Research Institute	SWAT / SRAC	JENDL-3.2
DTLR	Department for Transport Local Government and the Regions	WIMS	JEF-2.2
ORNL	Oak Ridge National Laboratory	BONAMI/NITAWL	238-energy-group
DEN/UFMG	Department of Nuclear Engineering/UFMG	NEWT/ORIGEN-S	V7-238-energy-group

6.2. SUPERCELLS EVALUATION WITH SPENT FUEL

The supercells using MOX, (Th-U)O_2-19.5%, (Th-U)O_2-16%, (TRU-Th)O_2 and (TRU-U)O_2 fuels were modelled. Figures 28 to 33 represent the supercell model using a quarter of MOX, (Th-U)O_2-19.5%, (Th-U)O_2-16%, (TRU-Th)O_2 and (TRU-U)O_2 and three-quarters of UO_2 fuel assemblies.

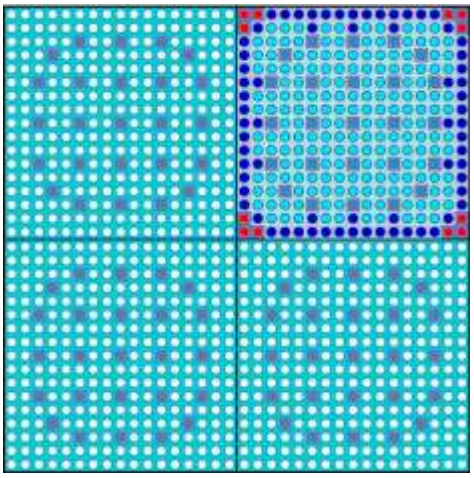

Figure 28 – MOX-UO_2 Supercell [author]

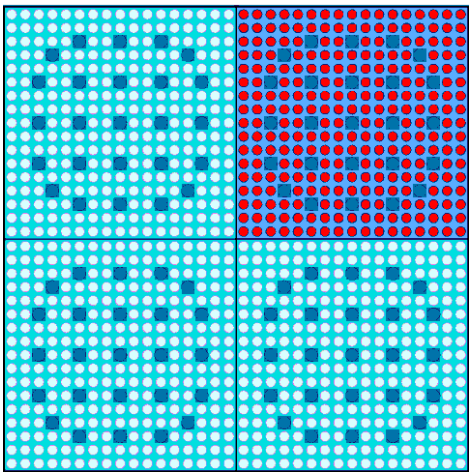

Figure 29 – (Th-U)O_2-19.5%-UO_2 Supercell [author]

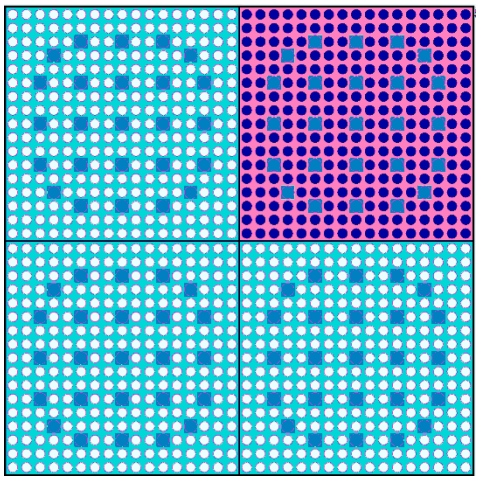

Figure 30 – (Th-U)O_2-16%-UO_2 Supercell [author]

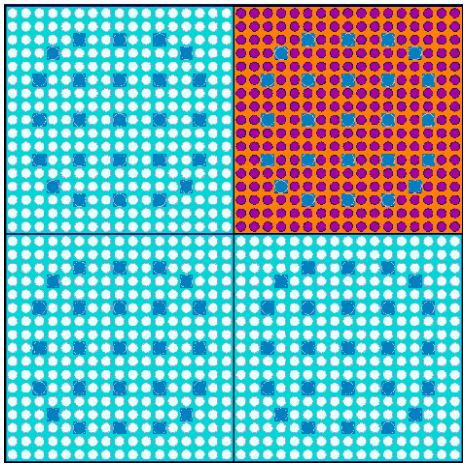

Figure 31 - (TRU-Th)O_2-UO_2 Supercell [author]

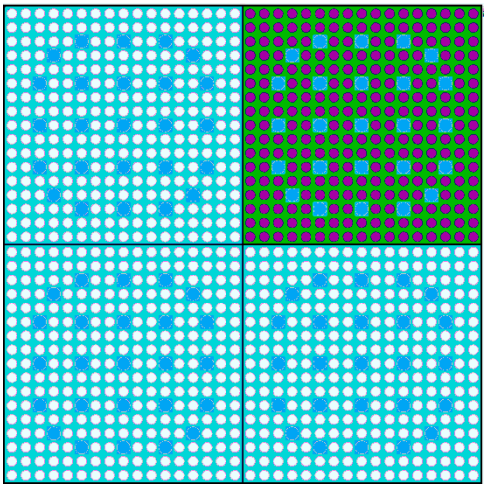

Figure 32 – (TRU-U)O_2-UO_2 Supercell [author]

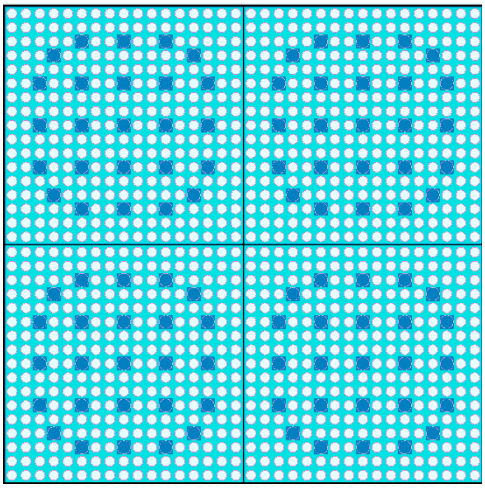

Figure 33 – UO_2 Supercell [author]

Another supercell model was evaluated considering a third of MOX, (Th-U)O_2-19.5%, (Th-U)O_2-16%, (TRU-Th)O_2 and (TRU-U)O_2 and two-thirds of UO_2 fuel assemblies. The study set this pattern following the various spent fuel patterns in the SFP storage racks [30]. Figures 34 to 39 represent the 1/3 supercells modelled.

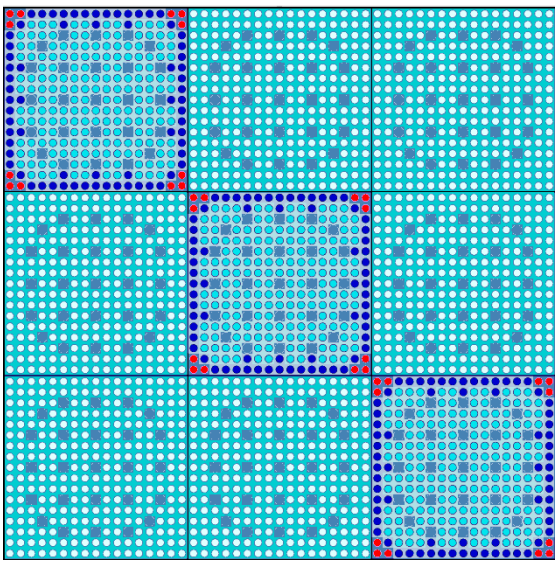

Figure 34 – MOX-UO_2 Fuel Supercell [author]

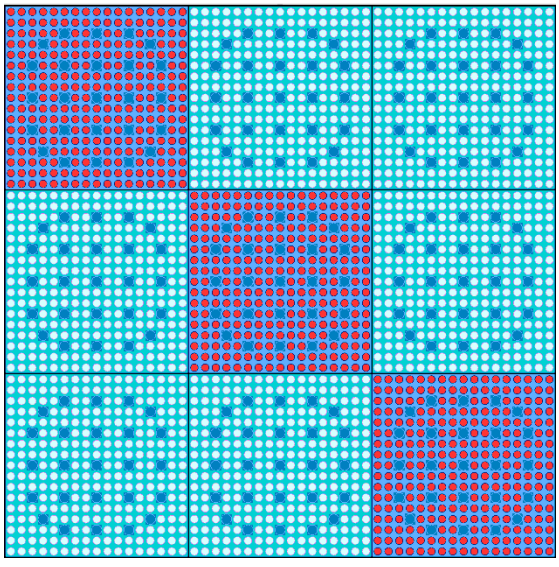

Figure 35 – (Th-U)O_2-19.5% -UO_2 Supercell [author]

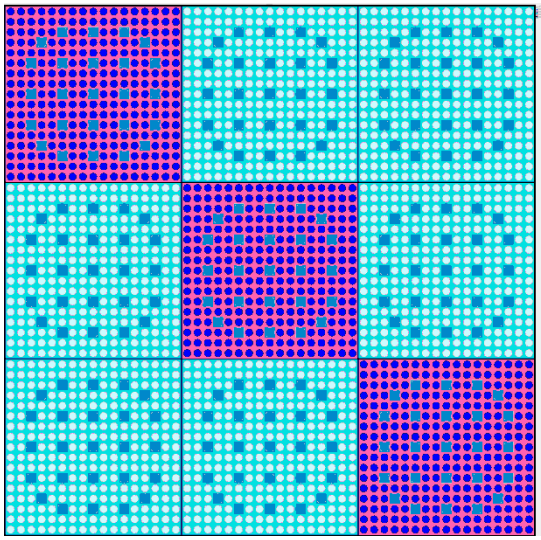

Figure 36 – (Th-U)O_2-16%-UO_2 Supercell [author]

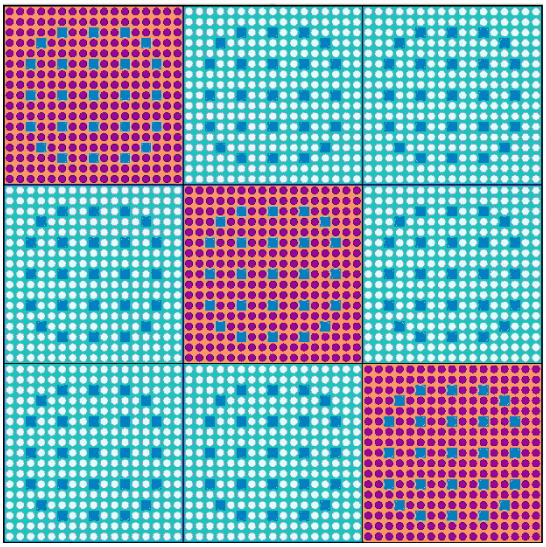

Figure 37 – (TRU-Th)O_2-UO_2 Supercell [author]

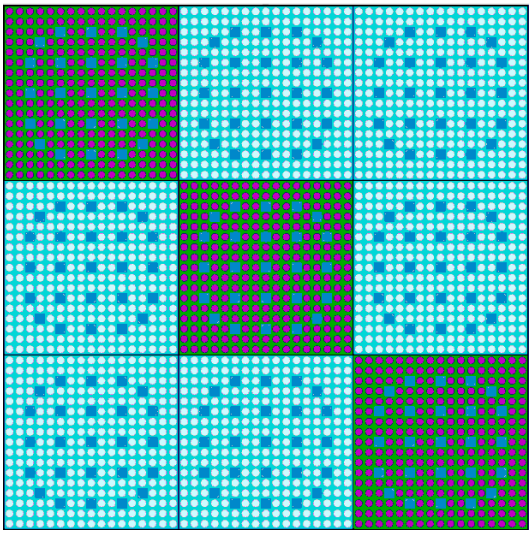

Figure 38 – (TRU-U)O_2-UO_2 Supercell [author]

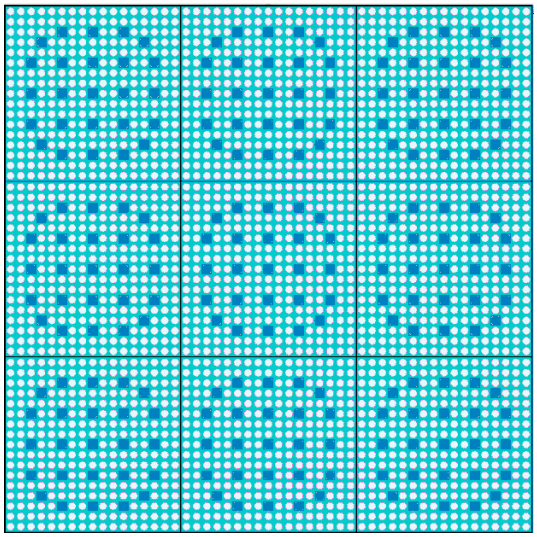

Figure 39 – UO_2 Supercell [author]

The supercells fuel compositions are the same adopted previously for the single assemblies. After setting all supercells' composition, the burnup criticality calculations were performed for all fuels.

The 1/4 and the 1/3 supercells were then modelled using the transport codes NEWT and validated with KENO-VI both in SCALE6.0.

6.3. SUPERCELLS BURNUP RESULTS

The TRITON module and the v7-238-energy-group library cross sections of the ENDF/B-VII library for 2000 generations and 2000 neutrons per generation package was used for the burnup. It was assumed an irradiation history with 3 cycles of 420 days and 38.09 MW/MTU density power was assumed [24]. The temperatures used were 900 K for the fuels, 620 K for the cladding and 575 K for the moderator [24]. The reactor operates with 600 ppm borated water [24] and the results were compared with those obtained for the UO_2 fuel.

Here, again the N = 3 was set for the parm = (addnux = N) allowing a more detailed configuration once that a total of 232 nuclides are followed during the burnup depletion. The k_{inf} evolution for the two supercells' configurations as a function of burnup is shown in Figures 40 and 41. Tables 38 and 39 represent the k_{inf} in the begin of life (BOL) as well as in the end of cycle 3 (EOC3) for the supercells using 3/4 and 2/3 of UO_2 fuel assemblies, respectively.

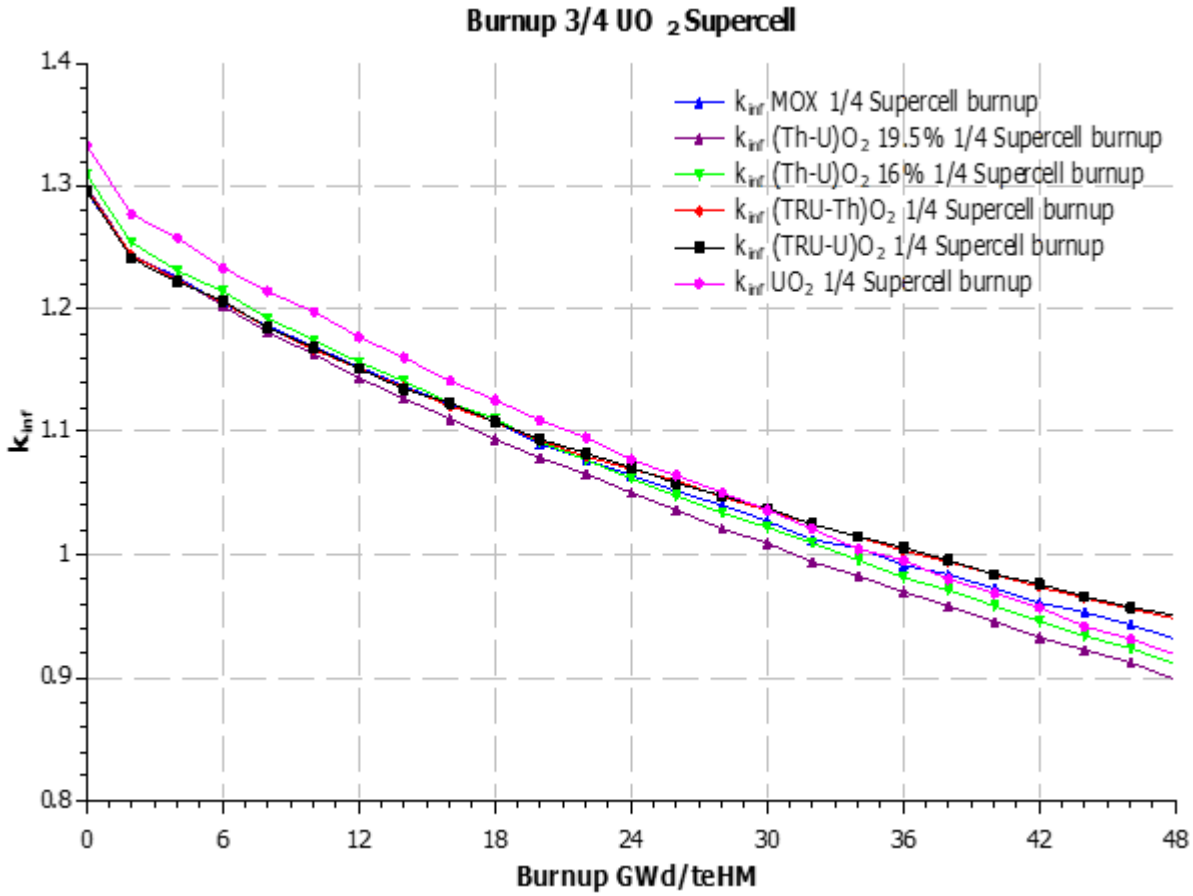

Figure 40 – k_{inf} evolution during the burnup for 3/4 UO_2 supercell with 1/4 of MOX, (Th-U)O_2-19.5%, (Th-U)O_2-16%, (TRU-Th)O_2 and (TRU-U)O_2

Table 38 – k_{inf} for the 3/4-UO_2 supercells burnup in the begin of life (BOL) and in the end of cycle 3 (EOC3)

Supercell	**k_{inf} in the begin of life**	**k_{inf} in the end of cycle 3**
UO_2 - UO_2	1.3338	0.9196
MOX - UO_2	1.2954	0.9322
(Th-U)O_2-16% - UO_2	1.3002	0.8990
(Th-U)O_2-19.5% - UO_2	1.3088	0.9111
(TRU-Th)O_2 - UO_2	1.2972	0.9480
(TRU-U)O_2 - UO_2	1.2966	0.9515

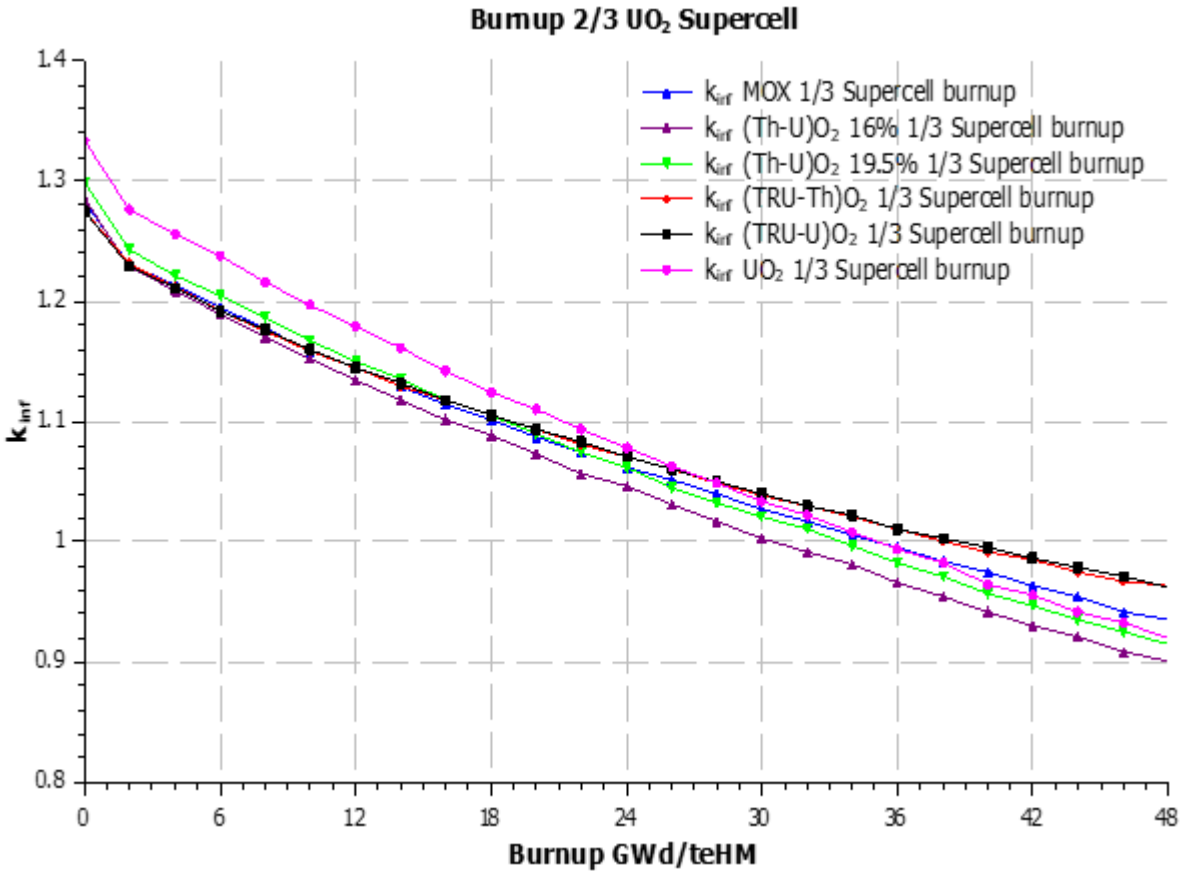

Figure 41 – k_{inf} evolution during the burnup for 2/3 UO_2 supercell with 1/3 of MOX, (Th-U)O_2-19.5%, (Th-U)O_2-16%, (TRU-Th)O_2 and (TRU-U)O_2

Table 39 – k_{inf} for all the 2/3 UO_2 supercell in the begin of life (BOL) and in the end of cycle 3 (EOC3)

Supercell	**k_{inf} in the begin of life**	**k_{inf} in the end of cycle 3**
UO_2 - UO_2	1.3330	0.9200
MOX - UO_2	1.2829	0.9353
(Th-U)O_2-16% - UO_2	1.2852	0.9006
(Th-U)O_2-19.5% - UO_2	1.2997	0.9145
(TRU-Th)O_2 - UO_2	1.2751	0.9628
(TRU-U)O_2 - UO_2	1.2747	0.9616

Figures 40 and 41 display a k_{inf} decrease more slowly when the (TRU-Th)O_2 and the (TRU-U)O_2 fuels are used in supercells together with UO_2 assemblies. This is expected because the production of ^{233}U compensates the burnup of fissile and fissionable isotopes. The (Th-U)O_2-19.5% and (Th-U)O_2-16% fuels have a high concentration of fertile ^{232}Th isotope and a considerable concentration of ^{238}U and ^{235}U. The ^{232}Th isotope increase the ^{233}U production over time while the ^{238}U and ^{235}U produce less of new fissile materials. Thus, it is ensured that the (Th-U)O_2-19.5% and (Th-U)O_2-16% fuel supercells have curves with a smooth slope, but not as much as the transuranic fuels' curve. The presence of fissile material such as the ^{239}Pu in MOX fuel makes possible to maintain the chain reaction, ensuring a smooth curve for this supercell.

When the supercells model is adopted, occurs a burnup extension once that the UO_2 fuel assemblies increases the amount of ^{238}U and ^{235}U present in the reactor core. Thus, less fertile and fissile isotopes are produced if (TRU-Th)O_2 or (TRU-U)O_2 fuel assemblies are introduced in the PWR core together with UO_2 fuel.

6.4. SUPERCELLS IN THE SPENT FUEL POOL

The safe criticality required was obtained for UO_2, MOX, (Th-U)O_2, (TRU-Th)O_2 and (TRU-U)O_2 fuels by inserting 313 supercells in the spent fuel pool. This amount of supercells was obtained considering the upper multiplication factor limit of 0.95 following the Final Safety Analysis Report [28] and the NRC regulation 10 CFR 50.68 [29]. The minimum pitch distance search was made by KENO-V sequence and CSAS5-S module in the SCALE 6.0 code. It was again verified that a 0.695cm pitch distance would maintain the criticality under the upper criticality limit of 0.95 and assure the maximum elements capacity in the SFP.

Table 40 summarizes the k_{inf} values for the 3/4-UO_2 supercell inserted in the spent fuel pool while Table 41 shows k_{inf} values for the 2/3-UO_2 supercells in SFP. The criticality was evaluated through KENO-VI sequence making use of CSAS6 module in the SCALE6.0 code and the v7-238-energy-group library.

Table 40 – Fuels initial k_{inf} when the 3/4 UO_2 supercells are inserted in the SFP

Supercell in SFP	**k_{inf}**
MOX - UO_2	0.79415 ± 0.00027
(Th-U)O_2-16% - UO_2	0.75561 ± 0.00022
(Th-U)O_2-19.5% - UO_2	0.77485 ± 0.00022
(TRU-Th)O_2 - UO_2	0.85679 ± 0.00025
(TRU-U)O_2 - UO_2	0.87086 ± 0.00031
UO_2 - UO_2	0.77860 ± 0.00025

Table 41 – Fuels initial k_{inf} when 2/3 UO_2 supercells are inserted in the SFP

Supercell in SFP	**k_{inf}**
MOX - UO_2	0.82245 ± 0.00027
(Th-U)O_2-16% - UO_2	0.75328 ± 0.00022
(Th-U)O_2-19.5% - UO_2	0.76826 ± 0.00024
(TRU-Th)O_2 - UO_2	0.86564 ± 0.00029
(TRU-U)O_2 - UO_2	0.87593 ± 0.00028
UO_2 - UO_2	0.77860 ± 0.00024

The multiplication factor values showed in Table 26 and Table 27 are in accordance with curves plotted in Figure 40 and Figure 41 once that follow the same k_{inf} descending order. The values are also in accordance with the k_{inf} values presented in Tables 20 and 21 when the assemblies are loaded in the mixed pool using different load patterns.

Mixing the standard UO_2 assemblies in the spent fuel pool together with MOX, (TRU-Th)O_2 or (TRU-U)O_2 supercells, made the criticality decrease. Even though criticality has increased when (Th-U)O_2-UO_2 supercells were inserted in the pool, for all the load cases, the $k_{safe} \leq 0.95$ requirement for the Spent Fuel Pool, remains guaranteed as established by Angra 2, Final Safety Analysis Report [28] and the NRC regulation 10 CFR 50.68 [29].

7. THE DELAYED NEUTRON FRACTION VARIATION DURING THE BURNUP

The delayed neutrons behavior was evaluated using all fuels in a PWR core. To validate the work using NEWT code, the results from fuel assemblies and supercells were compared with the previously results obtained with KENO-VI. After validating the NEWT model, this code will be used for all subsequent neutron transport calculations using the MOX, (Th-U)O_2-19.5%, (Th-U)O_2-16%, (TRU-Th)O_2 and (TRU-U)O_2 fuels.

The calculations for the fuel assemblies and supercells depletion were performed using module TRITON with KENO-VI code for the burnup and NEWT for the neutron transport. The k_{inf} values and the delayed neutrons fraction (DNF) were analyzed along the irradiation time. These calculations were performed at a constant power of 38.09 MW/MTHM for 1260 days and with two refueling activities after every 420 days. Figures 42 and 43 show the k_{inf} evolution for the assemblies and the 3/4-UO_2 supercells using all types of fuels, during irradiation. Table 42 and 43 represent the fuel assemblies k_{inf} as well as 3/4-UO_2 supercells k_{inf} in the beginning of life (BOL) and in the end of cycle 3 (EOC3).

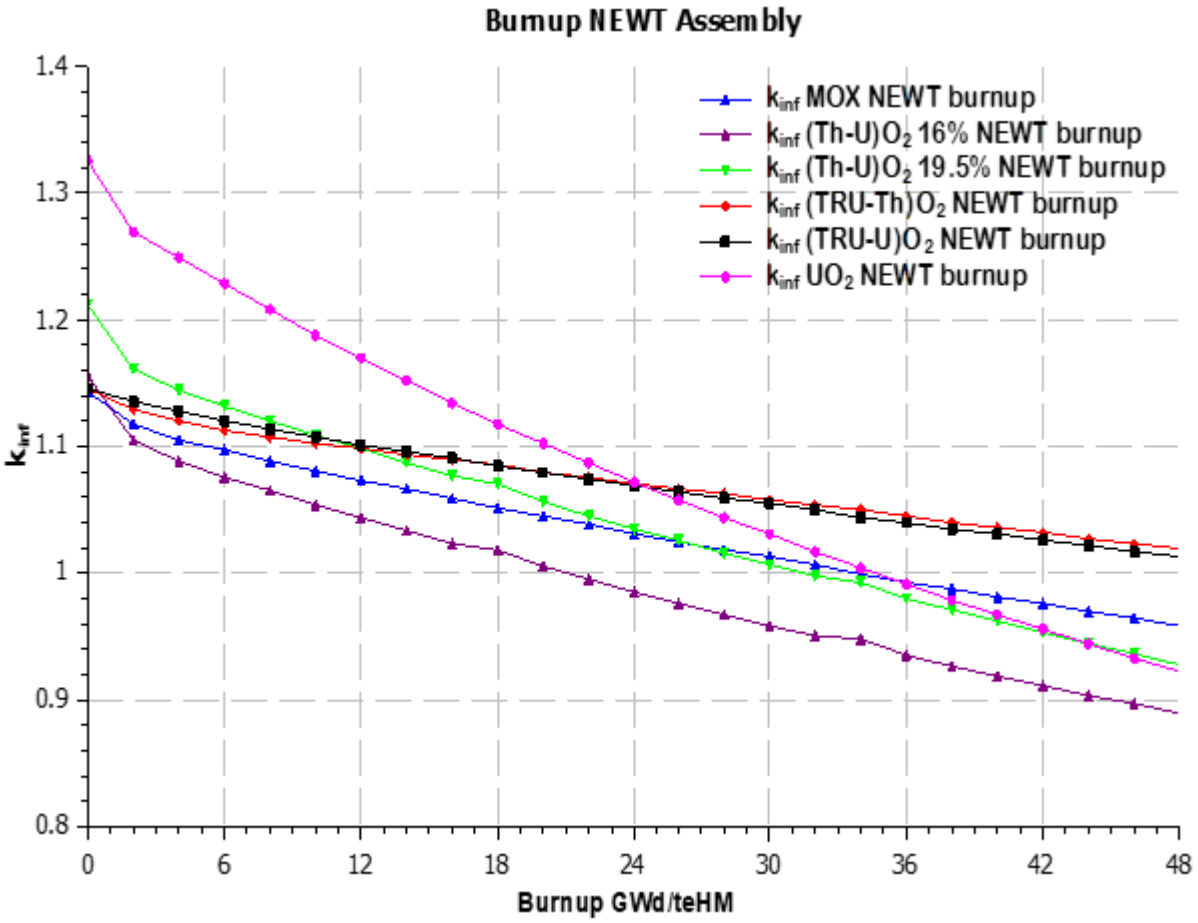

Figure 42 – k_{inf} evolution during the burnup for UO_2, MOX, (Th-U)O_2-16%, (Th-U)O_2-19.5%, (TRU-Th)O_2 and (TRU-U)O_2 assemblies

Table 42 – Fuel assemblies k_{inf} in the begin of life (BOL) and in the end of cycle 3 (EOC3)

Fuel	**Initial k_{inf} (BOL)**	**Final k_{inf} (EOC 3)**
MOX	1.1468	0.9586
UO_2	1.3264	0.9221
(Th-U)O_2-19.5%	1.2125	0.928
(Th-U)O_2-16%	1.1563	0.8896
(TRU-Th)O_2	1.1455	1.0192
(TRU-U)O_2	1.1464	1.0128

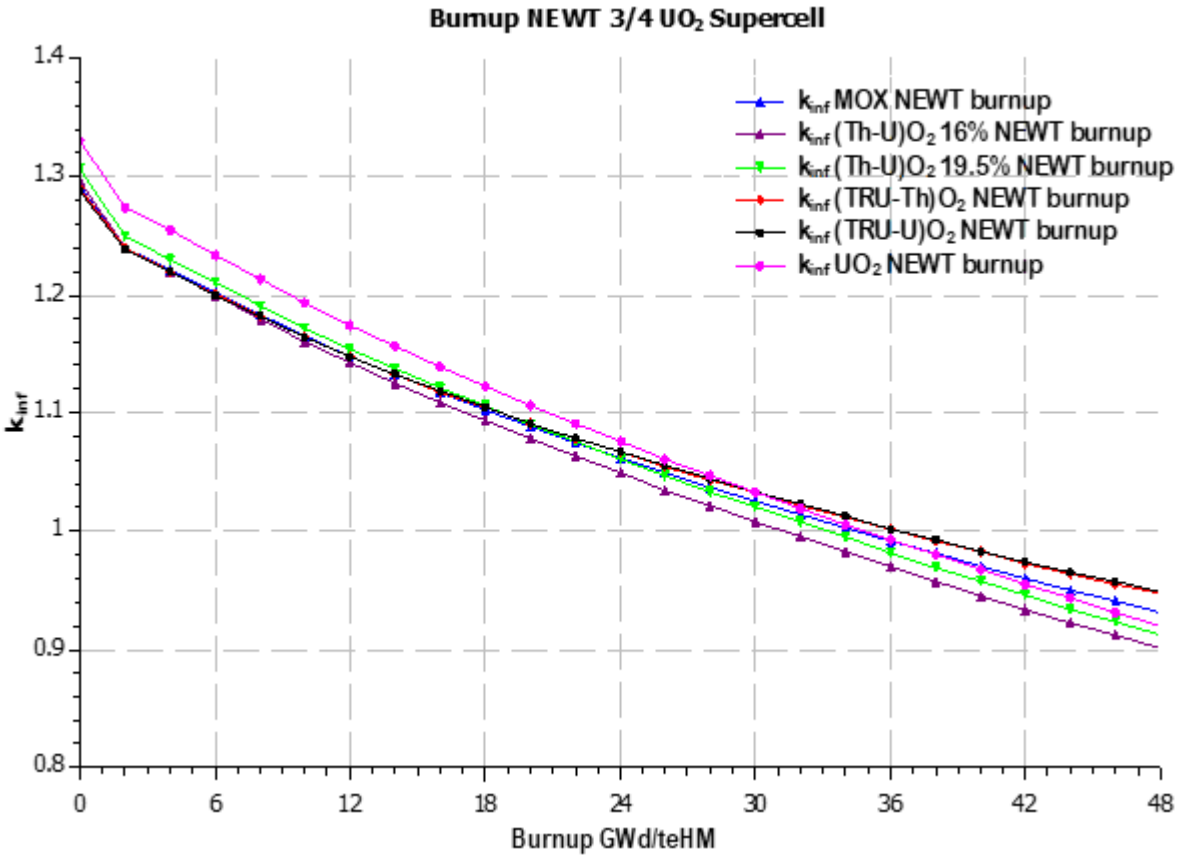

Figure 43 – k_{inf} evolution during the burnup for 3/4 UO_2 supercell with MOX, (Th-U)O_2-16%, (Th-U)O_2-19.5%, (TRU-Th)O_2 and (TRU-U)O_2

Table 43 – Fuel 3/4-UO_2 supercells k_{inf} for in the beginning of life (BOL) and in the end of cycle 3 (EOC3)

Fuel Supercell	**Initial k_{inf} (BOL)**	**Final k_{inf} (EOC 3)**
UO_2 - UO_2	1.3312	0.9201
MOX - UO_2	1.2920	0.9314
(Th-U)O_2-19.5% - UO_2	1.3065	0.9122
(Th-U)O_2-16% - UO_2	1.2969	0.9013
(TRU-Th)O_2 - UO_2	1.2898	0.9472
(TRU-U)O_2 - UO_2	1.2876	0.9487

The figures display a k_{inf} decrease more slowly when using the (TRU-Th)O_2 and the (TRU-U)O_2 fuels. This is expected because the production of ^{239}Pu compensates the burnup of fissile and fissionable isotopes in the reactor using a thorium-based fuel. The (Th-U)O_2-19.5% and (Th-U)O_2-16% fuels have a high concentration of fertile ^{232}Th isotope and a considerable concentration of ^{238}U and ^{235}U. The ^{232}Th isotope increase the ^{233}U production over time but the ^{238}U and ^{235}U do not give rise to new fissile materials. Thus, it is ensured that (Th-U)O_2 fuels have curves with a sharp slope curve. The presence of fissile material such as the ^{239}Pu in MOX fuel makes possible to maintain the chain reaction, ensuring a relatively smooth curve for this fuel.

Once that the supercells are used in the reactor core, there is a burnup extension possibility, mainly for (TRU-Th)O_2, (TRU-U)O_2 and MOX fuels. Therefore, it is feasible to use these fuels in the PWR core once mixed with standard UO_2 assemblies.

Figure 44 and 45 show a fuel assembly and a supercell according the mesh used by KENO-VI and NEWT. This configuration was used by KENO-VI for the model validation [24]. All the analysed assemblies and supercells have the same geometry, respectively 17x17 and 34x34.

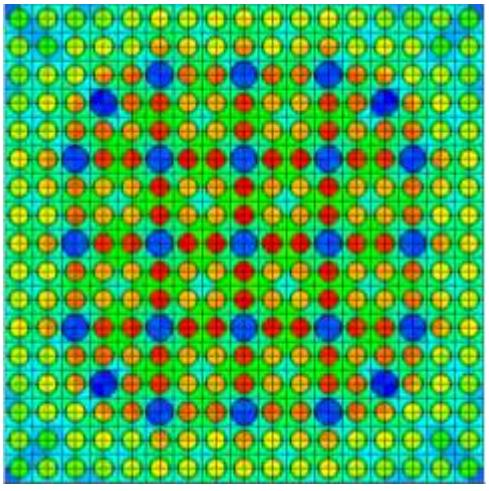

Figure 44 –Fuel assembly design generated by NEWT [author].

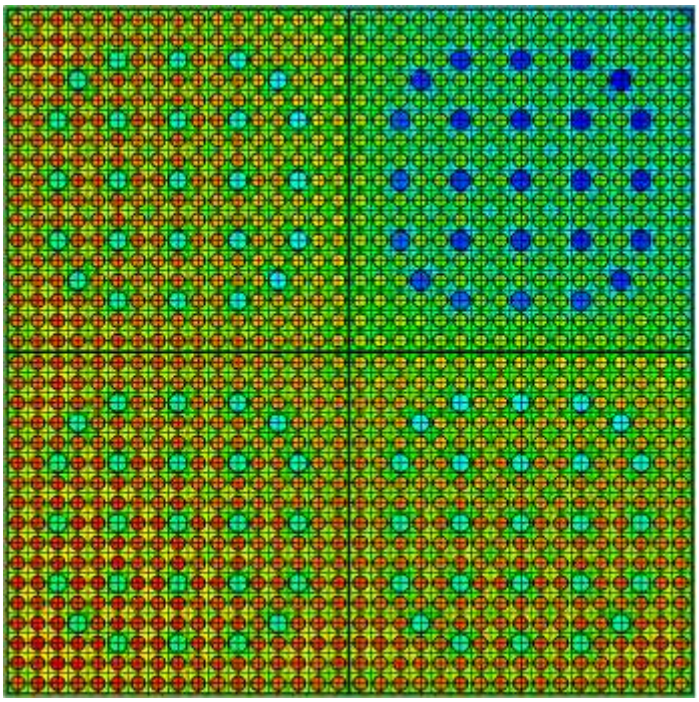

Figure 45 – 3/4 UO_2 supercell design generated by NEWT [author]

Tables 44 and 45 show the k_{inf}, calculated by KENO-VI (stochastic method) and NEWT (deterministic method) using the assemblies and the supercells. The values obtained display a close similarity between both codes. The small difference can be explained by the different methods used for each analysis. As the fissile material build up increases, the difference becomes larger, suggesting a correlation that can be further studied.

Table 44 – k_{inf} results by KENO-VI and NEWT for all fuel assemblies

Fuel	KENO-VI	NEWT	Absolute Differences (pcm)
MOX	1.1517 ± 0.0012	1.1468	490
(Th-U)O_2-19.5%	1.2147 ± 0.0012	1.2125	220
(Th-U)O_2-16%	1.1587± 0.0016	1.1563	240
(TRU-Th)O_2	1.1506 ± 0.0013	1.1465	410
(TRU-U)O_2	1.1534 ± 0.0013	1.1486	480
UO_2	1.3234 ± 0.0018	1.3264	300

Table 45 – k_{inf} calculated by KENO-VI and NEWT for the 3/4 UO_2 supercell load

Fuel	KENO-VI	NEWT	Absolute Differences (pcm)
MOX	1.2951 ± 0.0018	1.2920	310
(Th-U)O_2-19.5%	1.3102 ± 0.0015	1.3065	370
(Th-U)O_2-16%	1.3009 ± 0.0013	1.2969	400
(TRU-Th)O_2	1.2947 ± 0.0013	1.2898	490
(TRU-U)O_2	1.2914 ± 0.0015	1.2876	380
UO_2	1.3341± 0.0018	1.3312	290

Tables 44 and 45 present the selected cases using two different codes: KENO-VI and NEWT. To proceed with the validation, the k_{inf} absolute difference ($|k_{inf}$ KENO-VI - k_{inf} NEWT$|$) were measured, and only results with absolute difference lower than 500 pcm are considered. Therefore, these values are close enough to be considered satisfactory for the purpose of this work, which analyses the behavior of the fuels when using the assemblies and when a UO_2 assembly is replaced by a different fuel in the 3/4 UO_2 supercell configuration.

The delayed neutron fractions at BOL as well as at EOC 3 for all the fuel assemblies and supercells are presented in Tables 46 to 49.

Table 46 – Initial β calculated defining six effective groups of delayed neutrons for the different fuel assemblies

Initial delayed neutron fraction (β) – BOL						
Fuel	MOX	$(Th\text{-}U)O_2$-19.5%	$(Th\text{-}U)O_2$-16%	$(TRU\text{-}Th)O_2$	$(TRU\text{-}U)O_2$	UO_2
Total	3.37558E-03	6.90821E-03	6.93089E-03	2.40645E-03	2.95816E-03	7.17969E-03

Table 47 – Final β calculated defining six effective groups of delayed neutrons for the different fuel assemblies

Final delayed neutron fraction (β) – EOC 3						
Fuel	MOX	$(Th\text{-}U)O_2$-19.5%	$(Th\text{-}U)O_2$-16%	$(TRU\text{-}Th)O_2$	$(TRU\text{-}U)O_2$	UO_2
Total	3.78280E-03	4.46887E-03	4.21459E-03	2.64422E-03	3.15118E-03	5.06913E-03

According to Tables 46 and 47, for every fuel composition using the assemblies burnup model, the DNF is considerably smaller using the $(TRU\text{-}Th)O_2$ and $(TRU\text{-}U)O_2$ fuels, suggesting that a PWR reactor fueled with these type of fuels is more difficult to control than a PWR reactor fueled with the standard UO_2 fuel. It can be explained due to the strong influence of ^{239}Pu in the reprocessed transuranic fuels. The total β of ^{239}Pu isotope is $\beta = 0.0022$ in the thermal range, which is close to the obtained for the transuranic fuel assemblies [32].

For the $(Th\text{-}U)O_2$ fuel assemblies with 19.5 and 16% of fissile material, the DNF are close to the standard UO_2 fuel. The effective delayed neutron fraction for ^{233}U and ^{235}U are 0.00268 and 0.00665, respectively [32]. The decrease of ^{235}U and the increase of ^{233}U in the thorium-based fuels justifies the β results.

Table 48 – Initial β calculated defining six effective groups of delayed neutrons for the different 3/4 UO_2 supercell fuels

Initial delayed neutron fraction (β) – BOL						
Fuel	MOX	$(Th\text{-}U)O_2$-19.5%	$(Th\text{-}U)O_2$-16%	$(TRU\text{-}Th)O_2$	$(TRU\text{-}U)O_2$	UO_2
Total	7.18084E-03	6.89600E-03	6.91620E-03	7.18435E-03	7.18675E-03	7.16813E-03

Table 49 – Final β calculated defining six effective groups of delayed neutrons for the different 3/4 UO_2 supercell fuels

Final delayed neutron fraction (β) – EOC 3						
Fuel	MOX	$(Th\text{-}U)O_2$-19.5%	$(Th\text{-}U)O_2$-16%	$(TRU\text{-}Th)O_2$	$(TRU\text{-}U)O_2$	UO_2
Total	1.18019E-02	5.07457E-03	5.04967E-03	5.07009E-03	5.08295E-03	5.07000E-03

According to Tables 48 and 49, the DNF for every fuel is similar when the 1/4 Supercells burnup are evaluated in the PWR reactor. This suggests that a PWR reactor fueled with MOX, $(Th\text{-}U)O_2$-16%, $(Th\text{-}U)O_2$-19.5%, $(TRU\text{-}Th)O_2$ and $(TRU\text{-}U)O_2$ fuels together with UO_2 assemblies in a supercell model are approximately equal to control when the UO_2 fuel is used alone in the reactor core.

The delayed neutrons are responsible for the reactor response time, and during a transient, it is desired that this parameter is as high as possible, especially when positive reactivity is inserted. For small reactivity insertions, the reactor period is mainly determined by the average neutron lifetime, including delayed neutrons, while these neutrons can be neglected for large positive insertions. Along with these effects, each precursor decay constant is also significantly smaller when using the TRU fuels, which suggests a strong shift of the reactor period and response time. Tables 50 to 53 summarize the initial and final decay constant in the BOL and EOC 3 respectively for every fuel assemblies and supercells.

Table 50 – Initial Decay Constant defining six effective groups of delayed neutrons for all assemblies

Initial Decay Constant (λ) – BOL						
Fuel	MOX	$(Th\text{-}U)O_2$-19.5%	$(Th\text{-}U)O_2$-16%	$(TRU\text{-}Th)O_2$	$(TRU\text{-}U)O_2$	UO_2
Total	4.27557E+00	4.79956E+00	4.78063E+00	3.81710E+00	4.00274E+00	4.83588E+00

Table 51 – Final Decay Constant defining six effective groups of delayed neutrons for all assemblies

Final Decay Constant (λ) – EOC 3						
Fuel	MOX	$(Th\text{-}U)O_2$-19.5%	$(Th\text{-}U)O_2$-16%	$(TRU\text{-}Th)O_2$	$(TRU\text{-}U)O_2$	UO_2
Total	4.06902E+00	4.47245E+00	4.42444E+00	3.81566E+00	3.96888E+00	7.36715E+00

Table 52 – Initial Decay Constant defining six effective groups of delayed neutrons for the 3/4 UO_2 supercell fuels

Initial Decay Constant (λ) – BOL						
Fuel	MOX	$(Th\text{-}U)O_2$-19.5%	$(Th\text{-}U)O_2$-16%	$(TRU\text{-}Th)O_2$	$(TRU\text{-}U)O_2$	UO_2
Total	4.27190E+00	4.83020E+00	4.82994E+00	4.83544E+00	4.83614E+00	5.53911E+00

Table 53 – Final Decay Constant defining six effective groups of delayed neutrons for the 3/4 UO_2 supercell fuels

Final Decay Constant (λ) – EOC 3						
Fuel	MOX	$(Th\text{-}U)O_2$-19.5%	$(Th\text{-}U)O_2$-16%	$(TRU\text{-}Th)O_2$	$(TRU\text{-}U)O_2$	UO_2
Total	5.52970E+00	4.53457E+00	5.52872E+00	5.53599E+00	5.53872E+00	5.53265E+00

Figure 46 shows the DNF variation during burnup for all analyzed fuel assemblies. For MOX, (TRU-Th)O_2 and (TRU-U)O_2 fuels, there is a small increase on DNF value, while the DNF for the UO_2 and thorium-based fuels decreases more steeply, but maintaining their values always above the MOX and the transuranic fuels. This behavior can be explained due to the production of ^{233}U isotope, which has a low value of $\beta = 0.0026$, in both (Th-U)O_2 fuels, maintaining the DNF value stable [32]. Table 54 shows the initial and final DNF values for fuel assemblies during the burnup in a PWR reactor.

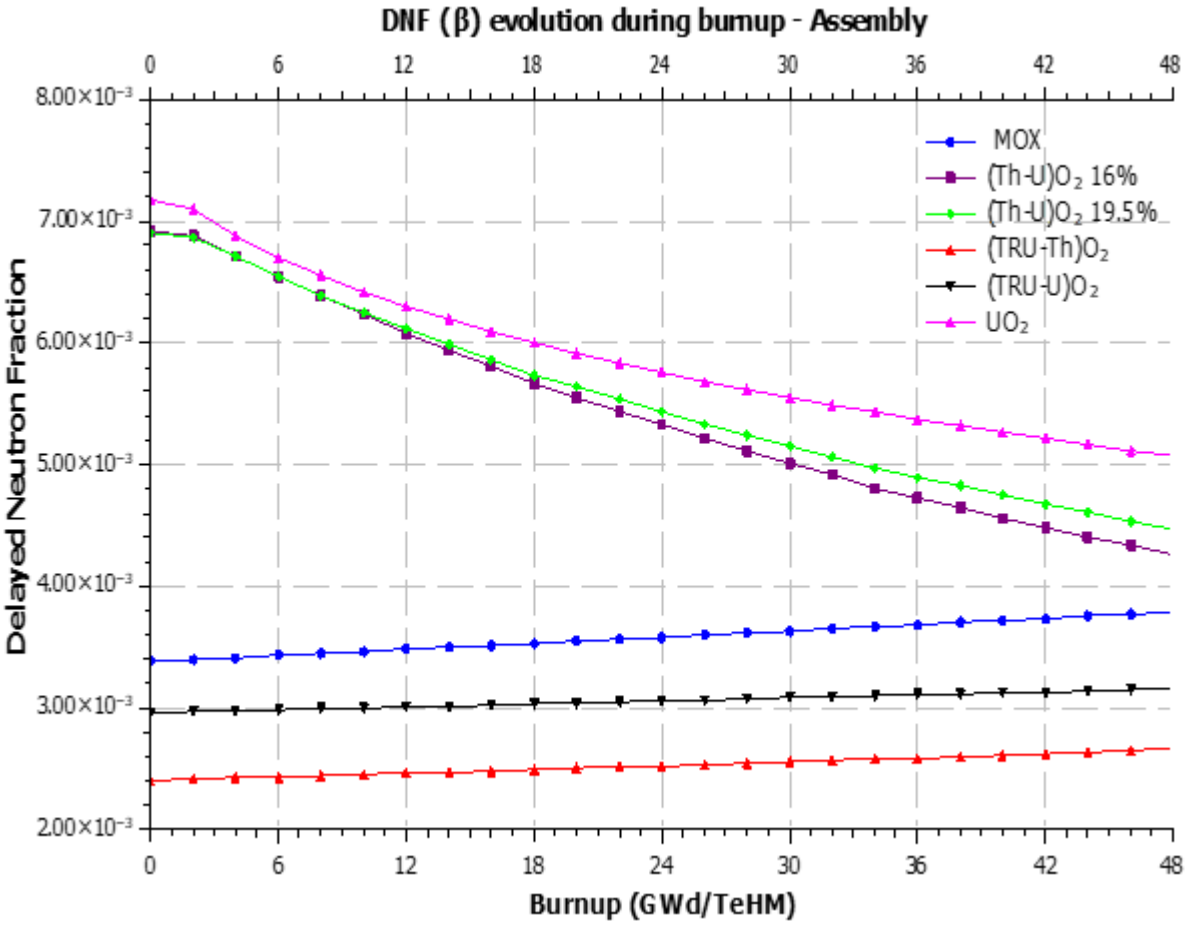

Figure 46 – DNF evolution during burnup for MOX, (Th-U)O_2-16%, Th-U)O_2-19.5%, (TRU-Th)O_2 and (TRU-U)O_2 assemblies

Table 54 – DNF for all the fuel assemblies in the begin of life (BOL) and end of cycle 3 (EOC3)

Fuel	**Initial DNF (BOL)**	**Final DNF (EOC 3)**
MOX	3.375E-03	3.782E-03
UO_2	7.179E-03	5.069E-03
(Th-U)O_2-19.5%	6.908E-03	4.468E-03
(Th-U)O_2-16%	6.916E-03	4.261E-03
(TRU-Th)O_2	2.406E-03	2.677E-03
(TRU-U)O_2	2.958E-03	3.151E-03

Figure 47 represents the DNF evolution when a 3/4 UO_2 supercell model is adopted in a PWR reactor. The high amount of ^{235}U in the supercell initial composition increase the DNF once that its delayed neutron fraction value is 0.00665. With the burnup evolution, the production of ^{233}U increase rapidly and for all fuel supercells a downline is verified. Table 55 shows the initial and final DNF values for fuel supercells during the burnup.

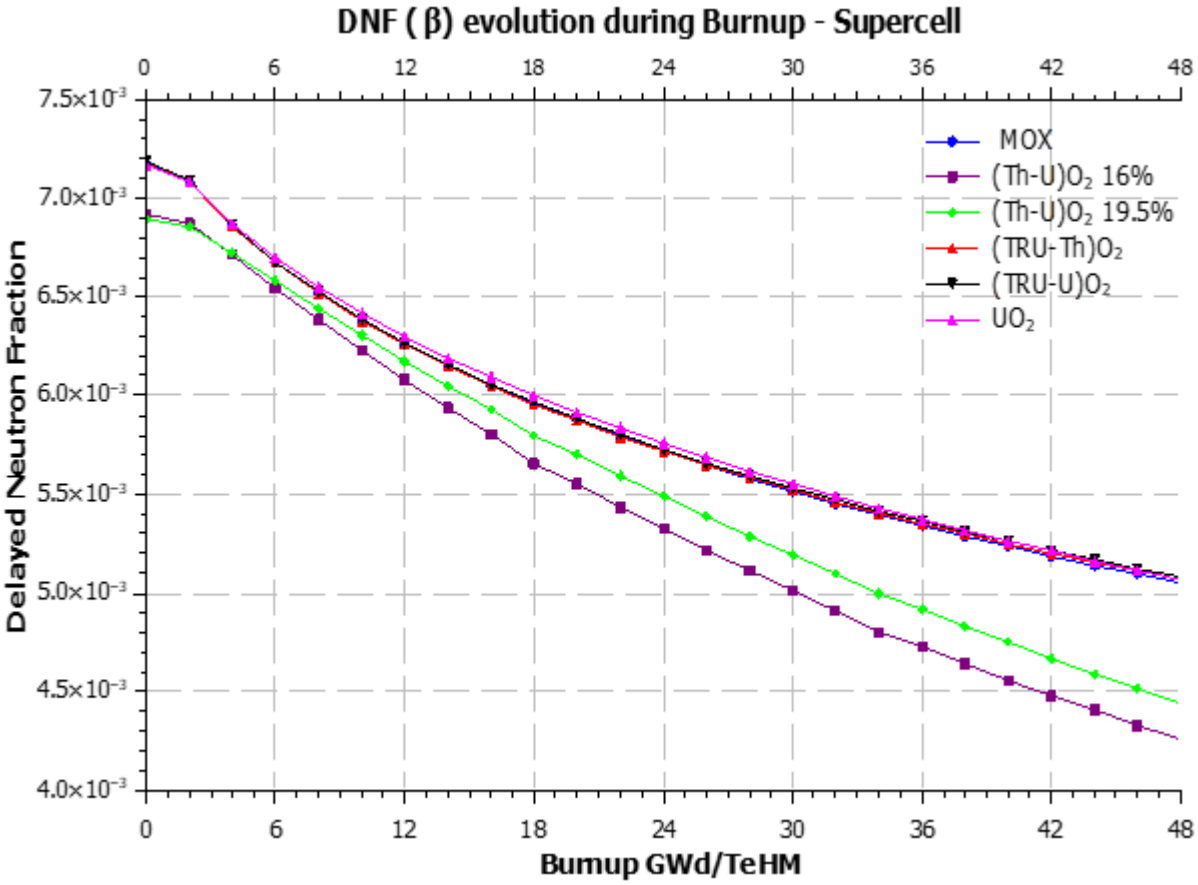

Figure 47 – DNF evolution during burnup for MOX, (Th-U)O_2-16%, Th-U)O_2-19.5%, (TRU-Th)O_2 and (TRU-U)O_2 supercells

Table 55 – DNF for all the fuel supercells in the begin of life (BOL) and end of cycle 3. (EOC3)

Supercell	**Initial DNF (BOL)**	**Final DNF (EOC 3)**
MOX- UO_2	7.180E-03	5.048E-03
(Th-U)O_2-19.5%-UO_2	6.896E-03	4.441E-03
(Th-U)O_2-16%-UO_2	6.916E-03	4.261E-03
(TRU-Th)O_2-UO_2	7.184E-03	5.073E-03
(TRU-U)O_2-UO_2	7.186E-03	5.082E-03
UO_2	7.168E-03	5.070E-03

8. GENERAL CONCLUSION AND FUTURE PERSPECTIVES

This study demonstrated the possibility to utilize MOX fuel, reprocessed transuranic fuel spiked with thorium, transuranic fuel spiked with uranium as well as thorium-based fuels in the PWR core once that they extends the burnup, decreases radioactive waste and decreases the risk of proliferation.

The alternative fuels showed a potential use and storage, maintaining the radioactive, decay heat, inhalation and ingestion radiotoxicity levels guaranteed for criticality accident requirements. Compared to uranium reactors, thorium reactors produce far less waste and the waste that is generated is much less radioactive and much shorter-lived.

A minimum pitch distance that optimizes the studied fuels insertion in the SPF keeping the system under the upper criticality limit was attained revealing that in no case, the pool needed to be resized.

The arrangement using a quarter either a third load pattern with MOX, (Th-U)O_2, (TRU-Th)O_2 or (TRU-U)O_2 fuels in the mixed-pools, showed a relevant criticality, radioactive, decay heat and radiotoxicities decrease.

The DNF for MOX, thorium- and uranium-transuranic fuels are considerably smaller than the UO_2. This is mostly due to a large amount of ^{239}Pu in the MOX and TRU fuels, that has a low value of total delayed neutrons, β $^{239}Pu = 0.0022$. In contrast, the presence of ^{235}U in the UO_2 fuel increases the total DNF of the system.

It is suggested that (TRU-Th)O_2, (TRU-U)O_2 and MOX fuels allow the burnup extension. The slow decrease of the fuel assembly's multiplication factor using the TRU fuels and MOX can be explained by the production of the ^{233}U fissile isotope presents in the ^{232}Th reaction chain. So, the burnup of the ^{239}Pu is compensated by the production of ^{233}U.

When using the (TRU-Th)O_2, (TRU-U)O_2 fuels, it is believed to be more difficult to have a reactivity control of the assembly. However, when the UO_2 supercell combined with these fuels is adopted it suggests the viability of using the reprocessed fuels in the PWR core.

The decay heat and the fuels' temperature variation in the Spent Fuel Pool are examples of new opportunities of study in the area.

Besides that, there exists the possibility to extend this work into cores analysis using reprocessed fuels. It also opens space to other concentration areas such as the thermohydraulic of the Th-U and TRU fuels.

REFERENCES

1. International Atomic Energy Agency, **Spent Fuel Reprocessing Options,** IAEATECDOC-1587, IAEA, 144 pp, Vienna, 2008.

2. AKBARI, Reza Jeyhouni; OCHBELAGH, Dariush Rezaei; MAIORINO, José Rubens; D'AURIA, Francisco; STEFANI, Giovanni Laranjo. **The utilization of Thorium in Small Modular Reactors – Part 1: Neutronic assessment**, Annals of Nuclear Energy. Volume 120, pp 422-430, Iran, 2018.

3. ORGANIZAION FOR ECONOMIC CO-OPERATION AND DEVELOPMENTECD/NEA, **Management of Recyclable Fissile and Fertile Materials.** NEA. No. 6107, 2007.

4. ORGANIZAION FOR ECONOMIC CO-OPERATION AND DEVELOPMENTECD/NEA, **Physics of Plutonium Recycling**. NEA. No. 6107, 2011.

5. PEREIRA, Claubia Lima; LEITE, Euzimar. **Non-Proliferating Reprocessed Nuclear Fuels in Pressurized Water Reactors: Fuel Cycle Options. Annals of Nuclear Energy**. Grã-Bretanha, v. 25, n.12, p. 937-962, 1998.

6. PEREIRA, Claubia Lima.; LEITE, Euzimar; FARIA, Eduardo. **Waste analysis generated by alternative reprocessing fuels from pressurized water reactions**. Annals of Nuclear Energy, v. 27, p. 449-464, 2000.

7. MONTEIRO, Fabiana; DE FARIA, Rochkhudson; FORTINI, Ângela.; DA SILVA, Clarysson; PEREIRA, Claubia. **Assessment of the Insertion of Reprocessed Fuels and Combined Thorium Fuel Cycles in a PWR System**. MRS Proceedings, v. 1769, p. IMRC 2014 6E-13, 2015.

8. MONTEIRO, Fabiana.; CASTRO, Victor; DE FARIA, Rochkhudson; FORTINI, M. Ângela; DA SILVA, Clarysson; PEREIRA, Claubia. **Micro Heterogeneous Approaches for the Insertion of Reprocessed and Combined Thorium Fuel Cycles in a PWR System**. MRS Proceedings, v. 1814, p. imrc2015sim28-abs012, 2016.

9. YAMATE, K.; ABETA. S.; SUZUKI, Keisuke. **MOX Fuel Design and Development Consideration**. Mitsubishi Heavy Industries Ltd, pp. 133-144, Yokohama, Japan, 1997.

10. ZHANG, Tianqi; YU, Shihe; CAO, Xinrong. **Research on the Loading Pattern of Reactor Core With MOX Fuel in the First Cycle**. ASME 2012 Power Conference, California, USA 2012.

11. NATARAJAN, Rajamani. **Reprocessing of spent nuclear fuel in India: Present challenges and future programme**. Department of Atomic Energy, Progress in Nuclear Energy, V. 101, pp. 118-132, India, 2017.

12. FUKUDA, K.; CHOI, J.-S.; SHANI, R.; DURPEL, L. V. D.; BEREL, E.; SARTORI, E., **MOX FUEL use as a Back-End Option: Trends, Main Issues and Impacts on Fuel Cycle Management**, International Atomic Energy Agency, IAEA-SM-358/I, Vienna.

13. MAIORINO, José Rubens; STEFANI, Giovanni Laranjo; MOREIRA, João; ROSSI, Pedro; SANTOS, Thiago. **Feasibility to convert an advanced PWR from UO_2 to a mixed U/ThO_2 core – Part I: Parametric studies**, Annals of Nuclear Energy, V. 102 pp. 47–55 2017.

14. AKBARI, Reza Jeyhouni; OCHBELAGH, Dariush Rezaei; MAIORINO, José Rubens; D'AURIA, Francisco; STEFANI, Giovanni Laranjo. **The utilization of thorium in Small Modular Reactors – Part I: Neutronic assessment**, Annals of Nuclear Energy, pp. 422–430, Tehran, Iran (2018).

15. GHOLAMZADEH Zohreh; FEGHHI, Seyed; SOLTANI, Leila; REZAZADEH, Marzieh; TENREIRO, Claudio, JOHARIFARD, Mahdi. **Burn-up calculation of different thorium-based fuel matrixes in a thermal research reactor using MCNPX 2.6 code**, De Gruyter, pp. 129-136, 2014.

16. INTERNATIONAL ATOMIC ENERGY AGENCY, **Thorium fuel cycle-potential Benefits and Challenges**. IAEA TECDOC-1450, IAEA, Vienna, 2005.

17. ORGANIZAION FOR ECONOMIC CO-OPERATION AND DEVELOPMENTECD/NEA, **Introduction of thorium in the Nuclear Fuel Cycle**. NEA No. 7224, France, 2015.

18. REARDEN, B. T.; JESSEE, M. A. **SCALE Code System**. ORNL/TM-2005/39, Version 6.2.1, Oak Ridge Laboratory, TN, EUA, 2016.

19. OAK RIDGE LABORATORY. **SCALE: A Modular Code System for Performing Standardized Computer Analyses for Licensing Evaluations**. ORNL/NUREG/CSD-2, Version 4.4, Volume 3, Washington, DC, 2000.

20. HOLLOENBACH, D. F; PETRIE, L. M. **CSAS6: Control Module for enhanced criticality safety analysis with Keno-VI**. Nuclear Science and Technology Division, Oak Ridge, Tennesse, USA, 2009.

21. DEHART, Mark. **TRITON: A two-dimensional transport and depletion module for characterization of spent nuclear fuel**, ORNL/TM-2005/39, Version 6, Volume I, Section T1, January 2009.

22. HOLLOENBACH, Daniel; PETRIE, Lester; LANDERS, N. F. **KENO-VI: A general quadratic version of the KENO program**, ORNL/TM-2005/39, Version 6, Volume II, Section F17, January 2009.

23. DEHART, Mark. **NEWT: A new transport algorithm for two-dimensional discrete ordinates analysis in non-orthogonal geometries**. ORNL/TM-2005/39, Version 6, Volume II, Section F21, January 2009.

24. O'CONNOR, Gregory; LIEM, Peng Hong. **Burn-up Credit Criticality benchmarck Phase IV – B: Results and Analysis of MOX Fuel Depletion Calculations**. Nuclear Energy Agency, France, 2003.

25. WEAVER, Kevan; ZHAO, Xianfeng; PILAT, Edward; HEJZLAR, Pavel. **A PWR Thorium Pin Cell Burnup Benchmarck**. INEEL-/CON 2000-00227, Idaho National Laboratory, 7-11 may, USA, 2000.

26. COTA, Stella; PEREIRA, Claubia. **Neutronic Evaluation Of The Nonproliferating Reprocessed Nuclear Fuelsin Pressurized Water Reactors**. Annals of Nuclear Energy, Grã-Bretanha, v.24, n.10, p. 829-834, 1997.

27. CASTRO, Victor; PEREIRA, Claubia. **Assessment of the insertion of the insertion of Reprocessed Fuel Spiked With Thorium in a PWR Core**, INAC-2017, Belo Horizonte, p. 22-27, 2017.

28. ELETRONUCLEAR - ELETROBRÁS TERMONUCLEAR S.A. **Final Safety Analysis Report** – FSAR Angra 2. Rio de Janeiro, Rev. 13, April, 2013.

29. U.S.NRC United States Nuclear Regulatory Commission. Protecting People and the environment Available on: ‹http://www.nrc.gov/reading-rm/doc-collections/cfr/part050/part050-0068.html› Accessed: 05,17,2019.

30. ORGANIZAION FOR ECONOMIC CO-OPERATION AND DEVELOPMENTECD/NEA; **Status Report on Spent Fuel Pools under Loss-of-Cooling and Loss-of-Coolant Accident Conditions**, Nuclear Safety NEA, CSNI/R(2015)2, May 2015.

31. BARTO, Andrew; CHANG, James; COMPTON, Keith; ESMAILI, Hossein. **Consequence Study of a Beyond-Design-Basis Earthquake Affecting the Spent Fuel Pool for a U.S. Mark I Boiling Water Reactor**. United States Nuclear Regulatory Commission, September 2014.

32. DUDERSTADT, James; HAMILTON, Louis. **Nuclear Reactor Analisys**. 2ª. ed. Michigan: Jon Wiley and sons, v. I, 1976.